A NEW FAMILY OF AIRFOILS BASED ON THE JET-FLAP PRINCIPLE

Andrew B. Bauer

Douglas Aircraft Company

Prepared for:

Office of Naval Research

September 1972

A NEW FAMILY OF AIRFOILS

BASED ON THE

JET-FLAP PRINCIPLE

UNCLASSIFIED

Security Classification

DOCUMENT CONTROL DATA · R&D

(Security classification of title, body of abstract and indexing annotation must be entered when the overall report is classified)

1. ORIGINATING ACTIVITY (Corporate author)

McDonnell Douglas Corporation
Long Beach, California 90846

2a. REPORT SECURITY CLASSIFICATION
UNCLASSIFIED

2b. GROUP

3. REPORT TITLE

A NEW FAMILY OF AIRFOILS BASED ON THE JET-FLAP PRINCIPLE

4. DESCRIPTIVE NOTES (Type of report and inclusive dates)

Technical Report, April 1971 through April 1972

5. AUTHOR(S) (Last name, first name, initial)

Bauer, Andrew B.

6. REPORT DATE	7a. TOTAL NO. OF PAGES	7b. NO. OF REFS
September, 1972	72	

8a. CONTRACT OR GRANT NO.	9a. ORIGINATOR'S REPORT NUMBER(S)
N00014-71-C-0250	
b. PROJECT NO.	
c.	9b. OTHER REPORT NO(S) (Any other numbers that may be assigned this report)
d.	

10. AVAILABILITY/LIMITATION NOTICES

Approved for public release; distribution unlimited

11. SUPPLEMENTARY NOTES	12. SPONSORING MILITARY ACTIVITY
	Office of Naval Research Aeronautics Code 461 Arlington, Virginia 22217

13. ABSTRACT

A new family of airfoils based largely on the utilization of the jet flap principle and termed Power Profiles was conceived by Mr. A. M. O. Smith of the Douglas Aircraft Company in 1970. In this report several unique features associated with this new concept, and the applicability of existing experimental data and theoretical methods to its evaluation, design and development are described. This technology is used to develop a configuration suitable for wind tunnel testing, and the report concludes with a discussion of those outstanding aerodynamic problems for which analytical and experimental research is required.

DD FORM 1 JAN 64 1473 0101-807-6800

UNCLASSIFIED

Security Classification

14. KEY WORDS	LINK A		LINK B		LINK C	
	ROLE	WT	ROLE	WT	ROLE	WT
Airfoil						
Jet Flap						
Wall Jet						
Coanda						
Circulation Control						
High Lift						
Drag						
Blowing						

INSTRUCTIONS

1. ORIGINATING ACTIVITY: Enter the name and address of the contractor, subcontractor, grantee, Department of Defense activity or other organization *(corporate author)* issuing the report.

2a. REPORT SECURITY CLASSIFICATION: Enter the overall security classification of the report. Indicate whether "Restricted Data" is included. Marking is to be in accordance with appropriate security regulations.

2b. GROUP: Automatic downgrading is specified in DoD Directive 5200.10 and Armed Forces Industrial Manual. Enter the group number. Also, when applicable, show that optional markings have been used for Group 3 and Group 4 as authorized.

3. REPORT TITLE: Enter the complete report title in all capital letters. Titles in all cases should be unclassified. If a meaningful title cannot be selected without classification, show title classification in all capitals in parenthesis immediately following the title.

4. DESCRIPTIVE NOTES: If appropriate, enter the type of report, e.g., interim, progress, summary, annual, or final. Give the inclusive dates when a specific reporting period is covered.

5. AUTHOR(S): Enter the name(s) of author(s) as shown on or in the report. Enter last name, first name, middle initial. If military, show rank and branch of service. The name of the principal author is an absolute minimum requirement.

6. REPORT DATE: Enter the date of the report as day, month, year; or month, year. If more than one date appears on the report, use date of publication.

7a. TOTAL NUMBER OF PAGES: The total page count should follow normal pagination procedures, i.e., enter the number of pages containing information.

7b. NUMBER OF REFERENCES: Enter the total number of references cited in the report.

8a. CONTRACT OR GRANT NUMBER: If appropriate, enter the applicable number of the contract or grant under which the report was written.

8b, 8c, & 8d. PROJECT NUMBER: Enter the appropriate military department identification, such as project number, subproject number, system numbers, task number, etc.

9a. ORIGINATOR'S REPORT NUMBER(S): Enter the official report number by which the document will be identified and controlled by the originating activity. This number must be unique to this report.

9b. OTHER REPORT NUMBER(S): If the report has been assigned any other report numbers *(either by the originator or by the sponsor)*, also enter this number(s).

10. AVAILABILITY/LIMITATION NOTICES: Enter any limitations on further dissemination of the report, other than those imposed by security classification, using standard statements such as:

(1) "Qualified requesters may obtain copies of this report from DDC."

(2) "Foreign announcement and dissemination of this report by DDC is not authorized."

(3) "U. S. Government agencies may obtain copies of this report directly from DDC. Other qualified DDC users shall request through _____."

(4) "U. S. military agencies may obtain copies of this report directly from DDC. Other qualified users shall request through _____."

(5) "All distribution of this report is controlled. Qualified DDC users shall request through _____."

If the report has been furnished to the Office of Technical Services, Department of Commerce, for sale to the public, indicate this fact and enter the price, if known.

11. SUPPLEMENTARY NOTES: Use for additional explanatory notes.

12. SPONSORING MILITARY ACTIVITY: Enter the name of the departmental project office or laboratory sponsoring *(paying for)* the research and development. Include address.

13. ABSTRACT: Enter an abstract giving a brief and factual summary of the document indicative of the report, even though it may also appear elsewhere in the body of the technical report. If additional space is required, a continuation sheet shall be attached.

It is highly desirable that the abstract of classified reports be unclassified. Each paragraph of the abstract shall end with an indication of the military security classification of the information in the paragraph, represented as *(TS)*, *(S)*, *(C)*, or *(U)*.

There is no limitation on the length of the abstract. However, the suggested length is from 150 to 225 words.

14. KEY WORDS: Key words are technically meaningful terms or short phrases that characterize a report and may be used as index entries for cataloging the report. Key words must be selected so that no security classification is required. Identifiers, such as equipment model designation, trade name, military project code name, geographic location, may be used as key words but will be followed by an indication of technical context. The assignment of links, roles, and weights is optional.

September 1972 Report No. MDC J5713

A NEW FAMILY OF AIRFOILS BASED ON THE JET-FLAP PRINCIPLE

by

A. B. Bauer

Prepared by the Douglas Aircraft Company
Long Beach, California, Under Contract
N00014-71-C-0250/NR 215-189/01-08-71 Code 461

for

Office of Naval Research
Aeronautics, Code 461
Department of the Navy
Arlington, Virginia 22217

jc

The development of a new family of airfoils based on the jet-flap principle as described in this report was performed by the Douglas Aircraft Company, Aerodynamic Research Group - Aerodynamics, of the McDonnell Douglas Corporation. A specific airfoil configuration suitable for development testing in the wind tunnel has been designed, and the report concludes with a discussion of those outstanding aerodynamic problems for which analytical and experimental research is required. The work was sponsored by ONR and was performed between April 1971 and April 1972 under Office of Naval Research Contract N00014-71-C-0250. The ONR Scientific Officer during this study was Mr. T. L. Wilson.

At the Douglas Aircraft Company this work was conducted by Dr. A. B. Bauer under the direction of Mr. M. L. Lopez (Principal Investigator) and Mr. A. M. O. Smith (Chief Aerodynamics Engineer for Research). A number of other people contributed to the work for which the author is grateful.

This report has been reviewed and is approved.

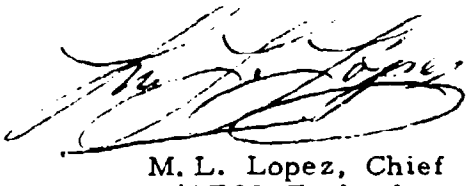

M. L. Lopez, Chief
V/STOL Technology Development Group

Date October 31st, 1972

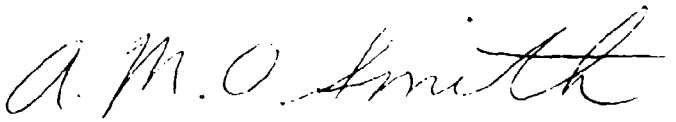

A. M. O. Smith
Chief Aerodynamics Engineer for Research

Date 31 October, 1972

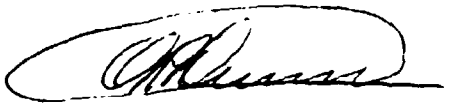

O. R. Dunn
Director of Aerodynamics

Date 13 October, 1972

TABLE OF CONTENTS

TABLE OF NOTATION

c	airfoil chord
h	height of tunnel test section
k	$\log_e 2$
$\dot{m}$	mass flow rate
n	exponent on Gartshore-Newman velocity profile
p_∞	free-stream static pressure
q_∞	free-stream dynamic pressure, $1/2\ \rho_\infty U_\infty^2$
s	distance along airfoil chord measured clockwise from the trailing edge
s_{ol}	value of s at front stagnation point
s_j	distance in chord lengths from aft end of a constant pressure region on an airfoil upper surface to the aft end of a constant pressure region on the airfoil lower surface
t	airfoil maximum thickness when used without subscript, jet slot or nozzle thickness when used with a subscript
u	local velocity in boundary layer or wall jet profile
x	airfoil coordinate parallel to the chord line
y	airfoil coordinate perpendicular to the chord line
y_m	distance from the wall to point of maximum u in the Gartshore-Newman wall-jet formulation
y_2	distance from the wall to the second point where $u = (U_e + U_m)/2$ in the Gartshore-Newman wall-jet formulation, see Figure 16
C_L	lift coefficient
C_{L_d}	design lift coefficient
C_p	pressure coefficient
C_μ	jet momentum coefficient, see Equation 1

C_μ'	modified C_μ, see Equation 3
$C_{\mu_{cr}}$	critical value of C_μ at which jet flap effects first begin, see Section 1
L_o	$y_2 - y_m$
M_∞	free-stream Mach number
Q_J	jet mass flow rate, $\rho_J U_J t_J$
Re_c	Reynolds number based on U_∞ and c
U	airfoil surface velocity neglecting boundary layer effects
U_c	value of U in a region where U is constant
U_e	velocity at the edge of the boundary layer
U_J	jet velocity at the slot exit plane
U_{J_∞}	velocity that the jet would attain if the jet air were expanded isentropically to P_∞
U_m	maximum value of u
U_{max}	maximum value of U
U_∞	free-stream velocity
V	U_c/U_∞
α	airfoil angle of attack
Γ_∞	airfoil circulation
δ_F	flap deflection angle
$\theta_{B.L.}$	boundary layer momentum thickness
θ_J	jet momentum thickness, see Equation 4
ρ_∞	free-stream density
ρ_J	density of jet flow at slot exit plane

Subscripts

l	on airfoil lower surface
u	on airfoil upper surface
J	jet, airfoil upper or lower surface not specified

A NEW FAMILY OF AIRFOILS
BASED ON THE JET-FLAP PRINCIPLE

1. INTRODUCTION

The term Power Profile was first used by Mr. A. M. O. Smith of the Douglas Aircraft Company to denote an airfoil type which requires the use of power under all flight conditions to avoid separation. Thus, it contrasts with ordinary airfoils, which use streamlining to avoid separation. The original use of the term referred to power applied by suction over a portion of the airfoil as well as blowing. However, as the investigation proceeded, the term was limited to airfoils with blowing only. The term is used in this same sense for the work reported here.

For a typical Power Profile shape, as originally conceived by Mr. Smith and as illustrated in Figure 1a, the power is applied by two wall jets emanating from the two slots near the profile trailing edge.* Because of the Coanda effect, the jets follow the rear surface to a stagnation point before merging into a single jet stream and leaving the profile. The two slots are located upstream of the points where the boundary layers on the upper and lower surface would otherwise separate, so that the jet entrainment may be used to avoid separation.

Review of Older Forms of Powered Airfoils. Before proceeding, a brief review of earlier forms of jet powered airfoils is needed for comparison to the Power Profile concept.

(a) Circulation Control. The idea of circulation control is illustrated in Figure 1b. This concept utilizes a jet to energize the upper surface boundary layer so that the flow separation point is moved around

*Patent protection is being sought by MDC on the device and system.

the trailing edge to some location on the airfoil lower surface. By this means the rear stagnation point also is moved to the lower surface with a large increase in C_L, the section lift coefficient. The location of the rear stagnation point and hence C_L is a function of C_μ, α, and Re_c. Unfortunately the lack of suitable analytical methods and experimental data prevents the prediction of C_L as a function of these parameters.

(b) The Pure Jet Flap. The jet flap is illustrated in Figure 1c. This is a conventional airfoil with a slot at the trailing edge so that a jet of air may be blown outward. The jet supplies a portion of the airfoil lift directly from the downward component of the jet momentum. The remainder of the jet flap lift comes from the interaction of the jet stream and the flow about the airfoil; this lift appears as a change in the airfoil pressure distribution.

(c) Circulation Control and Jet Flap Effects Combined. A configuration like that of Figure 1b may be operated as a circulation-controlled airfoil so long as the jet blowing coefficient C_μ does not exceed some critical value $C_{\mu_{cr}}$. When C_μ exceeds $C_{\mu_{cr}}$ the jet will leave the airfoil rear stagnation region with a total pressure greater than the free-stream total pressure. In this case a definite jet stream will exist akin to that of the pure jet flap. As a result, lift is generated by jet flap action as well as by the jet control of the rear stagnation point. On the other hand, a configuration like Figure 1c cannot be used in a circulation control mode because the jet blowing slot is not arranged to effect any significant change in stagnation point location.

(d) Airfoil and Flap With Jet Boundary Layer Control. Figure 1d shows a conventional airfoil and flap with jet boundary layer control. The jet energizes the air over the top surface of the flap so that separation can be avoided. The rear stagnation point is attached to the flap trailing edge and therefore moves with the flap deflection. Circulation control on this airfoil may be effected by moving the flap and hence the rear stagnation point.

(e) Early French Jet Flap. Figure 1e shows a configuration with two jets blowing over the control surface. As in Figure 1d, the jet flap effect is controlled by the strength of the jet blowing, and the rear stagnation point is changed by the control surface deflection.

History of the Application of Powered Airfoils. Many attempts have been made to utilize circulation-control and jet-flap systems on various research aircraft. Some of these are illustrated in References 1 and 2, but to the writer's knowledge such features have appeared only on a few military aircraft. The reasons for this appear to be tied to the problems of ducting air from an engine to the jet system, the added complexity of such a system, and the aircraft weight penalty associated with such systems. To overcome these problems, it is necessary to design the system into the aircraft from the very beginning. This requires a serious study of all the complex factors in the design process, and designers are not prone to accept novel ideas. Therefore, few such aircraft have been built. It is hoped that this situation can be corrected by utilizing the advantages of the Power Profile concept.

Advantages of Using the Power Profile Concept. The Power Profile concept has been developed around a number of ideas which lead to a number of advantages over the past powered airfoil systems. The main idea has been to use two wall jets near the airfoil trailing edge to prevent separation. By arranging the jet slots as shown on Figure 1a, the jets converge into a single jet at the rear of the control surface, as shown in Figure 2. By properly locating the control surface center of rotation, a small rotation of the control surface will simultaneously change the slot widths t_ℓ = EF and t_u = BC shown in Figure 2. Since t_ℓ grows larger as t_u grows smaller, one jet grows stronger and the other weaker as the control surface is deflected. This results in a change in location of the rear stagnation point D and hence a change in the airfoil C_L. By deflecting the surface fully so that either t_ℓ or t_u is zero, all the air will emanate from

the opposite slot, and the geometric configuration is then much like Figure 1b. For such a configuration Williams[3] obtained $C_L = 6.3$ using a jet momentum coefficient $C_\mu = 0.23$. Also, for $C_\mu = 0.23$ but for the control surface near its neutral position we would have $C_L \simeq 0$. That is, large changes in C_L can be obtained for only small control surface deflections. This feature is quite attractive for control purposes. Since $C_\mu = 0.23$ is relatively small, C_μ may be increased so that we also may expect C_L values greater than 6.3.

Based on these ideas and a careful contouring of the airfoil shape one finds that Power Profiles offer the following advantages over conventional airfoil sections:

(1) A better integration of the following systems:

(a) Cruise lift system with uniform chordwise loading.
(b) Cruise propulsion system with low drag.
(c) Control system.
(d) High-lift system.
(e) Engine-out control system.

This powered airfoil idea avoids separation, resulting in low drag in cruise. As discussed by Stratford[4,5], the "full thrust" should be realized, form drag should be removed, and aircraft drag reduction is crudely estimated to be at least five percent. The elimination of separation permits airfoil shaping to produce a uniform loading along the airfoil surface for some design or cruise C_L. On the other hand, high C_L is available for takeoff and landing; and control of C_L is done with only one control surface. The air supply from the several engines may be ducted together so that in case of an engine failure the air supply to all controls is still available from the remaining engines. In addition, the thrust from the remaining engines will be distributed more evenly than is possible if the engines are not ducted together.

(2) A Partial Integration of the Lift and Propulsion Systems. Only a part of the propulsion airflow from the engines should be needed to power the airfoil; by careful design the airflow required to provide high lift capability, to avoid separation, etc., may be minimized. This means that a minimum of ducting is required to carry air from engine nacelles to the wing sections. On the other hand, one can always envision a fully integrated system wherein all engines are buried inside the wing, but the size of engines seems to preclude th ea at present.

(3) Thick, Low Weight Airfoil Sections. Because of the separation control near the trailing edge, the trailing edge regions may be made much thicker than for conventional airfoils without a corresponding increase in airflow velocity around the airfoil. This gives an overall increase in airfoil thickness and volume which provides a better structure and might result in a net weight reduction. The airfoils that are worked out are the thickest possible for a given critical Mach number. Hence they contain the greatest volume and so offer the best possible solution to the internal ducting problem.

(4) Simple, Low-Weight Lift and Control System. A further weight reduction stems from the replacement of the conventional, rather complicated flap and aileron systems by the simple control surface shown in Figures 1a and 2.

(5) Low Control Surface Inertia. Because the control surface need move only a small distance for large changes in lift, and because the control surface is not large, the effective inertia of the control surface is quite small. This means that the control system can respond very quickly to control inputs. Such a quality is useful for gust alleviation. Ride quality is a critical problem on STOL aircraft[6]. Good use of the control surface might be found in active control system applications such as flutter prevention. Also, the control system response is so quick that it is not out of the question for helicopter applications. The system is as fast as any other jet flap system.

(6) High Lift Capability.

(7) Low Drag in Cruise.

(8) Better Transonic and Buffeting Characteristics. Because of separation control and the increased airfoil thickness near the trailing edge, the maximum air velocity over a Power Profile shape should be less than on a conventional airfoil of the same maximum thickness and lift. This is an important factor for increasing the critical Mach number and consequently reducing transonic buffeting and shock losses, if ducting problems are solvable.

(9) Negative Lift and Ground Thrust Reversal. After touchdown the control surface may be deflected upward quickly to provide large negative values of lift. Such negative lift would be useful after landing for improving aircraft braking effectiveness and for the drag associated with such lift. Furthermore, the Coanda effect may result in considerable thrust reversal action.

(10) Low Noise Characteristics. With regard to jet noise, Reference 7 shows that the jet flap system similar to Figure 1d is significantly quieter than the augmentor wing flap or the even louder externally blown flap. Part of this advantage is because of the shielding action of the flap. Reference 8 reports that the jet noise generally decreases with increase in the ratio of actual jet circumference to the circumference of the equivalent round jet of the same cross-sectional area. Thus, because the jet flap has a large circumference to area ratio, the jet flap noise generation should be importantly less than an equivalent circular jet.

With such attractive advantages in sight, the impact of the Power Profile concept on aircraft design could be quite substantial. Therefore, an important preliminary step is to substantiate these claims by means of both theoretical and experimental investigations. The first part of this step is carried out here in the form of a theoretical study of two-dimensional Power Profile characteristics.

2. PRELIMINARY DISCUSSION OF POWER PROFILE DESIGN

Two important requirements for this design are the capability for operation both at high-lift and at cruise conditions. This produces a conflict in selecting the basic airfoil shape so as to avoid adverse pressure gradients. To resolve this conflict, a basic airfoil shape is selected to avoid adverse gradients at cruise or low C_L configurations. Although cruising flight may be done transonically, for the present first cut subsonic techniques will be used to gain experimence. Then the cruising shape used at high C_L and the resulting adverse gradients are accepted as the price to pay for a desirable pressure distribution at cruise. At high C_L, C_μ is much higher than for cruise C_L, and the flow should still be unseparated.

Design for High Lift Conditions

Both Williams[3] and Kind and Maull[9] have discussed the adverse pressure gradients associated with thick, powered airfoils under high-lift conditions. The pressure distributions on the upper surface have a "saddleback" shape, with large peaks near the leading and trailing edges (much like those on Figure 14). The recovery from the aft peak may be taken care of by the wall jet at that location, so only the front peak is of concern. For such a gradient, Stratford's criterion[10] for turbulent boundary layers indicates no separation, at least up to C_L's of the order of 6.0. At low Reynolds numbers a laminar bubble may form and burst, causing trouble, but this should be no trouble at flight Reynolds numbers where the boundary layer almost surely is turbulent.

Williams[3] reports a $C_{L_{max}}$ of 6.3 at a value of blowing coefficient C_μ equal to 0.23. Here

$$C_\mu = \frac{Q_J U_{J_\infty}}{q_\infty c} \tag{1}$$

where Q_J is the jet mass-flow rate, U_{J_∞} is the velocity that the jet would attain if expanded isentropically to the free-stream pressure, q_∞ is the free-stream dynamic pressure, and c is the airfoil chord.

The essential control and high lift features of the Power Profile have been illustrated by Werle[11], who shows flow visualization results obtained in a water channel, using the shape illustrated in Figure 3. Although Werlé varied the momenta of the two jets by varying the plenum pressure of the two jets independently rather than by varying t_ℓ and t_u, his results show the Coanda effect and the change in rear stagnation point location with change in jet momenta. These results also show the expected changes in direction of the merged jet downstream of the stagnation point. Unfortunately, Werlé does not report on the lift coefficient, which probably was not measured.

From these experimental results one expects that powered airfoils having a thickness/chord ratio of 0.20 or more and moderate camber should be capable of C_L's of 6.0 for $\alpha = 0$ degrees and for $C_\mu \approx 0.23$. For such a thickness/chord ratio and moderate camber we now may inquire as to the shapes of interest for low C_L or cruise conditions.

Design for Cruise Conditions

This problem may be idealized by first assuming the flow to be inviscid so that no boundary layer would develop and no separation would occur even without the use of the trailing edge jets. Then we should pick a profile shape such that for a given thickness we have surface velocities which are as small and as uniform as possible. The reason for wanting these small velocities is to minimize drag or to delay drag rise in the real application of the profile shape, where skin friction and high speeds are important. If flight is pushed well into the transonic region it may prove better to have a different pressure distribution, just as Whitcomb does. If so, that too can be designed into these shapes.

This requirement is illuminated by considering free-streamline shapes, examples of which are given in Figures 4 and 5. Free-streamline shapes have the remarkable property that the surface velocity is constant everywhere except for small regions near the stagnation points. A long time ago (Reference 12) the Douglas Aircraft Company worked out a very complete

set of solutions for incompressible flow; two of these are shown by Figures 4 and 5. Both of these shapes have free-streamline upper and lower surfaces with U_{max}/U_{∞}, the ratio of maximum velocity to free-stream velocity, equal to $\sqrt{1.50}$. These free streamlines run between the short, straight lines at the leading and trailing edges. In Figure 4 the straight lines are at a 45° wedge angle to the chord line; in Figure 5 this angle was chosen as 90°.

The value of this free-streamline analysis may be demonstrated by Figure 6, which compares a free-streamline shape with a conventional airfoil. The free-streamline shape is formed by two 75° half-angle wedges connected by two free streamlines chosen so that $(U_{max}/U_{\infty})^2 = 1.300$, and hence the pressure coefficient, C_p, is -0.300. A comparable airfoil is the NACA 65-012 because its thickness is sufficient to make $(U_{max}/U_{\infty})^2 = 1.357$, or somewhat larger than the free-streamline shape (Reference 13). Hence, the thicker, free-streamline shape has a smaller U_{max}/U_{∞} than the airfoil. The reason for this is clear; because the free-streamline shape has a constant U_{max}/U_{∞} over most of its length, whereas the airfoil has a more peaked U/U_{∞}, the average thickness of the free-streamline shape is larger than on the airfoil. This is related to the fact that the airfoil streamlining requirement forces the airfoil to be thin near the trailing edge, whereas the free-streamline shape is thick near the trailing edge. Because an airfoil is so thin near the trailing edge, the gains in cross-sectional area are even greater than the gains in thickness.

The above discussion is based on U/U_{∞} calculations for inviscid, incompressible flow. In real life the shapes will develop boundary layers which modify the results; the chief change will be the necessity for jet power to be applied to the free-streamline shape to avoid separation.

Other free-streamline shapes, ellipses, and airfoils are compared in Figure 7. This figure shows clearly that the free-streamline

shapes and the ellipses have a much larger thickness than the NACA airfoils for a given value of superstream velocity. For example, for $(U_{max}/U_{\infty})^2 = 1.5$ the NACA 66 series airfoil is 17.1 percent thick whereas the 90° free-streamline shape has a thickness ratio of 24.9 percent, which is 46 percent larger. In Figure 8 the same sections are compared on the basis of mean airfoil thickness rather than maximum thickness as in Figure 7. On the basis of mean thickness the free-streamline shapes are even more outstanding; for $(U_{max}/U_{\infty})^2 = 1.5$ the 90° free-streamline shape is 82 percent thicker than the NACA 66 series airfoil. Mean thickness is a convenient measure of the internal area, which is important to any ducting problem.

These examples were calculated for incompressible flow, but the same general ideas apply to subsonic and transonic flows. For transonic flows it is obvious that the free-streamline idea for minimization of local flow velocity is desirable. Unfortunately, a method is not currently available to carry out calculations of transonic airfoil shapes which have free-streamline surfaces.

It is interesting to take a Whitcomb type of airfoil, as shown in Figure 9, and to reshape the aft end, which was done starting at the 58.5 percent chord point and ending with the new trailing edge located at the old 66.0 percent chord line. The new airfoil has the same general shape as the free streamline shapes of Figures 4 or 6. Thus, the Whitcomb airfoil has been shortened considerably by using two wall jets rather than streamlining to pull together the flow over the upper and lower surfaces, thereby avoiding flow separation. Hence, the Power Profile drag should be less than that of the original Whitcomb section, since separation drag and some skin friction drag have been eliminated.

3. OBJECTIVES OF THIS STUDY

The main objectives of the present study have been to review and to assess the available theoretical methods and experimental data which apply to the Power Profile concept, and to plan for future action in the development of this concept. In particular, means of preventing separation, reducing drag, and obtaining high propulsion efficiency have been stressed. Theoretical methods are reviewed in Section 4 below, experimental data are reviewed in Section 5, and plans for future development of Power Profiles are given in Section 6.

4. THEORETICAL METHODS FOR POWER PROFILE DESIGN

From a theoretical viewpoint, the Power Profile design task is that of developing a powered airfoil which has the above-stated advantages over a conventional airfoil or jet flap. The task is one of using both viscous flow methods for the boundary layers and wall jets and inviscid methods for the potential flow regions. Methods that are of prime interest and that are needed for the job are described below.

Airfoil Shape, the Design C_L, and the James Method

If we specify that the airfoil upper surface has a constant velocity equal to V_u times U_∞, and that the lower surface velocity is V_ℓ times U_∞, then the design C_L will be

$$C_{Ld} = V_u^2 - V_\ell^2 \qquad (2)$$

Then the question arises as to how we pick V_ℓ and V_u for a given C_{Ld}. The answer in principle is quite simple. For a given C_{Ld} we may pick any V_ℓ and then solve equation (2) for V_u. Then it turns out that the airfoil thickness ratio t/c obtained is a function of V_ℓ; increasing V_ℓ will increase t/c, and vice versa.

This point may be better understood through a study of Figure 10. The two airfoil shapes in Figure 10 were generated by use of the James design (inverse) method[14]. The James method is a very powerful means of airfoil design wherein the airfoil theory is formulated in a transformed space consisting of the interior of the unit circle. In the practical application of the method the computer input information is a dimensionless plot of velocity V versus distance s along the airfoil perimeter, as illustrated in Figure 11. The output is then an airfoil shape and a pressure or velocity distribution which, in general, is slightly different from the input distribution. The reason for this difference, if any, is the physical impossibility of obtaining an airfoil which satisfies both potential flow theory and any input velocity distribution. Therefore, as discussed in detail in Reference 14, the James method is formulated to pick the airfoil that in some sense comes "nearest" to having the input velocity distribution. Figure 11 shows both distributions for the case 7 airfoil shown in Figure 10.

Since the James' method neglects viscosity and boundary layers, it is only approximately applicable to real flows. Hence, it applies to this approximation for the circulation control range, where $C_\mu \leq C_{\mu_{cr}}$, but for larger values of C_μ, where the jet flap effect is important, it no longer applies.

The airfoils on Figure 10 are two of a series of potential flow shapes calculated for use in the Power Profile development. Inasmuch as both airfoils have almost constant C_p values over most of their upper and lower surfaces, the surface velocities are almost constant and are listed non-dimensionally in Figure 10 as V_ℓ and V_u. Also, the airfoil C_L value for stagnation point locations shown on Figure 10 are listed; notice that C_L is approximately equal to the $(V_u^2 - V_\ell^2)$ given by equation 2 as the design C_L for the idealized case where the velocity distributions are constant over the entire chord length. For obvious reasons, the velocities generally will not be constant over the entire chord length, but Figure 10 shows the remarkable result that the velocities may be constant over as much as 95 percent

of the chord length. Other cases have shown that this number may be as much as 97 percent for an airfoil having t/c = 0.225; Pierce et al[12] have shown free-streamline shapes where the ratio is 100 percent. However, these larger numbers are not available for shapes having rounded leading edges such as those in Figure 10.

Equation 2 gives a rather good approximation to C_L for such cases as shown in Figure 10 partly because the difference $(C_{p_\ell} - C_{p_u})$ near the leading and the trailing edges is almost equal to its mid-chord value.

As illustrated on Figure 11, the case 7 input values of V_ℓ and V_u were 1.077 and 1.323. For case 9, the same V_ℓ and V_u were input. The output difference between the two cases, as shown in Figure 10, is the result of input differences of V versus s in the regions close to the leading and trailing edges, that is, near s = 0, 0.5, and 1.0. For these regions, the input slope dV/ds was larger by a factor of 1.62 in case 7 as compared to case 9. As a consequence, the case 9 airfoil turns out to be much thicker than that of case 7. Thus, by varying this slope one changes the output values of both V_ℓ and V_u.

A change in the input values of V_ℓ and V_u will no doubt have some effect on the James method output, but clearly the output is quite sensitive to dV/ds near the leading and trailing edges. To date, no calculations have been made on cases similar to 7 or 9 but with V_ℓ and V_u made larger or smaller.

The airfoil camber and lift coefficient may be varied by changes in the relative magnitudes of the inputs V_ℓ and V_u, which is comparable to displacing upward or downward the input curve of Figure 11. For symmetric airfoils and $C_L = 0$ one must use $V_\ell = V_u$ and V(0.500) = 0.

In some cases the output value of s_{01}, the value of s at the leading edge where U = 0, is significantly different from the input s_{01}. This

results in some output nonuniformity ("roundedness") in the two regions over which V is supposed to be constant, either V_ℓ or V_u. The output becomes flatter or more uniform in these regions when a more realistic value is picked for the input s_{01}.

The above is written with the implication that only one value of C_L is associated with any given airfoil. So far as the James method is concerned, this is true, since the James program puts out only one shape and one value of C_L. Of course, on any real airfoil we may then vary the angle of attack α and the circulation Γ to change C_L, but in so doing the flatness of the pressure and velocity distributions as exemplified by Figures 10 and 11 will be lost.

The James method is capable of generating airfoil shapes for almost any rational form of pressure distribution rather than just the class restricted to almost constant values of upper and lower surface velocity, as discussed above.

In summary, the James method is a very powerful means for generating potential flow shapes for application to Power Profile designs. Practical designs can be developed from the shapes like those in Figure 10 by modifying the trailing edge regions to accommodate the two jets and the control surface that characterize the Power Profile concept. Then, except for boundary layer displacement effects which can be compensated for, the flow over all but the rearmost part of the profile should have the pressure and velocity distribution given by the James method.

Douglas Neumann Method for Potential Flow Analysis

This method for potential flow calculations[15] is complementary to the James method discussed above, since it is a "direct" rather than an "inverse" method. The Douglas Neumann method has been developed for calculating the incompressible potential flow about arbitrary body shapes.

Hence, for practical applications, it is limited to cases where $C_\mu \leq C_{\mu_{cr}}$ since, like the James method, it does not account for viscosity or jet flap effects.

The means of solution, which is based on fundamental theorems of classical potential theory, utilizes a distribution of source density over the body surface and solves for the distribution that makes the normal component of fluid velocity equal to zero on the body surface in the presence of a given uniform stream. This approach is general, and does not make use of any simplifying assumptions. In particular, the body is not required to be slender, and perturbation velocities due to the body are not required to be small. Both interior and exterior flows can be calculated, and multiple-body interference problems present no difficulty. The theory and the details of the method are contained in Reference 15. Only a brief outline of the approach is given here.

The body surface is approximated by a large number of surface elements whose characteristic dimensions are small compared to those of the body. A two-dimensional or an axisymmetric body is specified by a single profile curve. This profile curve is approximated by a polygon consisting of a large number of short straightline segments, which in general are of unequal length. Thus the surface elements for two-dimensional bodies are thin, infinite plane strips, and those for axisymmetric bodies are frustums of cones having small slant heights. For three-dimensional bodies the surface elements are small plane quadrilaterals, which are distributed over the entire surface. On each element a control point is selected where velocities and pressures are to be evaluated. For two-dimensional and axisymmetric bodies the control points are the midpoints of the line segments that approximate the profile curve of the body.

The method basically consists of simultaneously adjusting the source densities on all the surface elements in such a way that the zero normal-velocity condition is satisfied at all control points. Specifically, the

method proceeds as follows. The surface source density is assumed to be constant over such surface element. Thus there is a number of unknown values of source density equal to the number of surface elements. The velocities induced by the elements at each other's control points are computed. Because of the linearity of the problem, the velocity at any point due to an element is proportional to the unknown value of source density on that element and is thus the product of this unknown value and the velocity at the point in question due to a unit value of source density on the element. It is required that the normal velocity at each control point due to all the elements equal the negative of the normal component of the onset flow there, so that the total normal velocity is zero. Application of a normal velocity condition at all control points produces a determinate set of linear algebraic equations for the values of source density on the elements. Once these equations have been solved, velocities and pressures are computed at the control points off the body surface in the flow field.

The Douglas Neumann program may be applied directly to airfoil shapes such as given in Figure 10 to determine pressure and velocity distributions as functions of both angle of attack and circulation, whereas the James method gives information for only one angle of attack and one circulation value. Therefore, to obtain both the airfoil shape and all possible pressure and velocity distributions, both the James and the Neumann programs must be used.

Since airfoils such as given in Figure 10 do not have a sharp trailing edge, no trailing edge or Kutta condition can be applied to define a unique value of circulation corresponding to each angle of attack. Therefore, the flow field is a function of both the angle of attack and the circulation, which for the Power Profile is controlled by the control surface deflection and the blowing strength. In applying the Neumann program the circulation is determined by the location of the rear stagnation point, which is specified as a program input. Hence, a unique flow field calculation depends on both the angle of attack and the rear stagnation point location.

The Neumann program also may be used to study incompressible potential flow about the control surface region of a Power Profile shape. This has been done using 40 points to define the control surface shape, 100 points to define the upper portion of the Power Profile and 100 points to define the lower portion of the Power Profile. For these 240 points the time required to run the program on an IBM 360/65 computer was 4.5 minutes. In this amount of time the computer obtained one solution at zero angle of attack, one solution at 90° angle of attack, and a circulatory solution. These solutions were combined by the computer to give a final solution at a specified angle of attack and with one stagnation point on the control surface, one stagnation point at the trailing edge of the upper surface, and one stagnation point at the trailing edge of the lower surface. Usually a smaller number of points is sufficient to obtain accurate results[15].

For a simpler shape such as shown on Figure 10, about 120 points are sufficient to define the airfoil with good accuracy. The computing time on an IBM 360/65 machine is then about 1.0 minute. The James design method on the same machine requires about 0.8 minute and provides data at 201 points on the body surface.

The Douglas Non-Linear "Jet Flap" Potential Flow Method

This method of calculating the inviscid, incompressible flow about multi-element airfoils is currently being developed under the sponsorship of the McDonnell Douglas Corporation Independent Research and Development Program. It is basically a surface-vorticity potential flow method, in which the surface of the airfoil and jet are replaced by a distribution of vorticity of such strength as necessary to make these surfaces streamlines of the flow. The calculation of the vorticity distribution is complicated by the fact that the jet location is not known in advance. The jet, which is required to extend downstream to infinity, must also satisfy a dynamic boundary condition relating to the curvature of the jet to the pressure difference across it. These mixed boundary

conditions make a direct solution by matrix techniques impossible; hence an iterative procedure is resorted to. A jet shape is initially estimated and the potential flow about the airfoil-jet combination is calculated. The resulting jet loading is compared to the value required to satisfy the dynamic boundary condition and, if a pre-specified tolerance is exceeded, the jet shape is modified. The potential flow calculation is repeated, and the dynamic boundary condition checked, until convergence is achieved. An operational computer program is presently available to perform the above calculations, and will soon be extended to include the effects of jet thickness and entrainment.

Use of the Above Methods. The above three methods may be classified as follows:

Methods for $C_\mu \leq C_{\mu_{cr}}$	Methods for $C_\mu > C_{\mu_{cr}}$
1. James	1. The Douglas Non-Linear "Jet Flap" Potential Flow Method
2. Neumann	

These methods are all for inviscid, incompressible flows, although the James method has recently been extended to handle certain compressible problems up to transonic speeds.

Boundary Layer Methods. Boundary layer calculations generally are not essential to the design of Power Profiles since it is not necessary to know the precise form of the boundary layer profile or other boundary layer parameters. In practical applications the boundary layers will be turbulent over most of the airfoil, and the use of Power Profiles with zero pressure gradient over most of surface simplifies the boundary layer to the well-known flat plate case. Therefore, the essential boundary layer characteristics may be approximated by the flat-plate results of Schlichting[16].

For more-detailed investigations the reader is referred to the work of Cebeci, Smith, and Wang[17], which is both up-to-date and old enough

to be well-tested. This is a finite-difference method for solving laminar- and turbulent-boundary-layer equations for incompressible and compressible flows about two-dimensional and axisymmetric bodies and contains a thorough evaluation of its accuracy and computation-time characteristics. The Reynolds shear-stress term is eliminated by an eddy-viscosity concept, and the time mean of the product of fluctuating velocity and temperature appearing in the energy equation is eliminated by an eddy-conductivity concept. The turbulent boundary layer is regarded as a composite layer consisting of inner and outer regions, for which separate expressions for eddy viscosity are used. The eddy-conductivity term is lumped into a "turbulent" Prandtl number that is assumed to be constant.

The method has been programmed on the IBM 350/65 under the name E7ET, and its accuracy has been investigated for a large number of flows by comparing the computed solutions with test data. On the basis of these comparisons, it can be said that this method is quite accurate and satisfactory for both laminar and turbulent flows. The computation time is also quite small. In general, a typical flow, either laminar or turbulent, consists of about twenty x-stations. The computation time per station is about one second for an incompressible laminar flow and about two to three seconds for an incompressible turbulent flow on the IBM 360/65. Solution of the energy equation in either laminar or turbulent flows increases the computation time about one second per station.

Boundary Layer Separation. Boundary layer separation should not be tolerated on useful airfoil, jet flap, or Power Profile sections. Several methods of predicting separation are compared for accuracy by Smith[18]. In particular, the Stratford criterion[10] is quite useful because it does not require the solution of the boundary layer equations. The best prediction method is that of Cebeci-Smith[19,20], but Head's method is not far behind. In general, for Power Profiles operating at the design C_L, separation will be no problem except in the immediate neighborhood of the control

surface, and this problem depends partly on the wall jet blowing and entrainment for its solution.

Wall Jet Methods. The wall jet and the mixing of the wall jet with the external boundary layer is of prime importance in Power Profile design. This is because of the use of the jets to prevent separation. The technology of jet attachment and the jet entrainment of the outside flow is less well understood than the other aspects of Power Profile aerodynamic design. Nevertheless, a number of papers on the wall jet have appeared in recent years.

Glauert[21] was the first to obtain a solution for a wall jet with no external stream; he treated both laminar and turbulent flows. Kruka and Eskinazi[22] have studied the turbulent case with external flow and zero pressure gradient and have found similarity to exist in both the inner and the outer parts of the wall-jet layer. Their results are based on their own experiments as well as those of others. Abramovich[23] gives a basic derivation of the development of the initial parts as well as the main regions of both submerged jets and wall jets; however, his wall jet work is limited to regions of zero pressure gradient Harris[24] has developed an integral calculation method for the turbulent problem with an arbitrary pressure gra the external stream; he compares calculated results with the me ts by himself and by others.

Newman . put forth an extensive review of recent wall jet work. Gartshore[26] has reviewed work on the blowing required to suppress separation, discussing the work of Thomas[27], and has touched briefly on a problem of importance to the Power Profile concept, namely whether or not a velocity defect, such as that in the initial mixing region of the wall jet and the external stream, is likely to deepen. This discussion is limited to small values of the velocity defect, whereas for Power Profiles, as with any wall jet in an external stream, the defect is large, initially corresponding to the jet trailing edge value of zero. This defect can

disappear rapidly, as will be discussed under Section 5. Gartshore and Newman[28] have worked together to develop a wall jet calculation procedure for arbitrary pressure gradients.

This method is the best currently available, although it has a number of simplifying assumptions which may be questioned. The calculation is based on four integral equations. The initial profile downstream of the jet slot is taken to be of a universal form defined by four parameters. Two of these parameters are chosen at the outset, and the remaining two are determined from mass and momentum conservation. In cases where this leads to a velocity profile with a maximum U_m greater than the jet velocity U_J in the slot, U_m is chosen to be equal to U_J, and the fourth parameter is determined by momentum conservation only. Predictions of the method have been compared with measurements on wall jets in various adverse pressure gradients, and the agreement between theory and experiment has been found to be satisfactory.

Gartshore and Newman have found that although the momentum coefficient C_μ may be adequate to describe the blowing momentum for large values of U_J/U_e, a more appropriate parameter must be devised for other cases. Calculations for two cases studied show that the excess momentum coefficient,

$$C'_\mu = C_\mu \left(1 - \frac{U_\infty}{U_J}\right) \tag{3}$$

first suggested by Kelly[29], satisfactorily collapses the data for low jet velocities or large slot widths, as may appear on Power Profiles.

The Gartshore and Newman method has been applied, and some results are discussed in Section 6.

Analysis of a Circulation-Controlled Elliptical Airfoil. Ambrosiani and Ness[30] have made an ambitious effort in developing a calculation

method for a circulation-controlled elliptical airfoil, such as shown in Figure 1b. It would be interesting to have their calculations compared with experimental results, but this has not yet been done, to this writer's knowledge. For generality, the calculations should be compared to experiment for several combinations of α, C_μ, t_u, and Reynolds number. It would also be well if the method could be adapted to other than elliptical shapes. Some parts of the analysis could be improved. For example, on pages 47-48 the theory of the extent of the pressure feedback zone is rather rough for Point A. On page 31 the transition criteria by Michel or by Granville would have been better. The jet mixing on page 56 is rather simplified. In general, the report is well-organized and is a useful beginning to the complete circulation-controlled airfoil problem.

A rather elegant general discussion of jet flaps has been given by Maskell and Gates[31]. In particular, they give a theorem showing for inviscid flows without shocks that the total resultant force on the two-dimensional airfoil is the vector sum of the lift, $\rho_\infty U_\infty \Gamma_\infty$, and the jet momentum, $\dot{m}\, U_{J_\infty}$, where $\dot{m}$ is the mass flow rate and U_{J_∞} is the jet velocity far behind the airfoil, which is always parallel to U_∞.

5. REVIEW OF EXPERIMENTAL CIRCULATION CONTROL AND JET FLAP DATA

Although the history of circulation-control and jet-flap airfoil data covers more than two decades, the main experimental efforts have been rather scattered, inasmuch as no definite airfoil type has been used as yet on more than a very few experimental aircraft. As a result, the experimental data is rich in the variety of airfoil types tested, but poor in detailed investigations of any particular type. Many tests have been performed on a scale such that Re_c, the Reynolds number based on chord length, is only about 10^6 or less. Of all the work reported here[32-47], only one test was conducted with Re_c greater than 6×10^6. Hence, there is yet much to learn from future powered airfoil experiments.

Wall-Jet Experiments. The wall-jet is essential to the operation of the Power Profile concept, since a wall jet is used to prevent separation over the rear of the airfoil. The wall jet must overcome the very strong adverse gradient at the rear of the airfoil; a second complication is the normal pressure gradient, the effect of which is not well understood. Hence, experiments are needed for a better understanding of this problem.

The wall-jet problem has been studied in part by Jones[32], who has measured a large number of wall-jet velocity profiles on the rear of a kind of airfoil with a constant 20 percent chord thickness except for rounded leading and trailing edges, as illustrated on Table I. Jones has run tests with one jet placed just upstream of the trailing edge. The jet travels somewhat more than 90° around the trailing edge before separation. This may be compared with the data on curved wall jets presented by Newman[25]. The Newman study contrasts to the above because Newman's results are for the case where the external stream velocity is zero, so that U_J/U_∞ is infinity rather than 2 to 4, as in the Jones study. Hence, it is not surprising that Newman predicts the much larger turning angle of 226° before separation.

During the experiments[32], Jones never was able to cause the upstream boundary layer to separate from the jet flow before the jet itself separated from the surface. This was true in spite of deliberate attempts to generate such a separation.

The absence of such a possible separation is important to the success of the Power Profile concept. Therefore, the several papers[33,34,48] which show measurements of the merging of wall jets with upstream boundary layers are of special interest. No separation was found in these measurements, even for adverse pressure gradients[48]. These results are encouraging, particularly because the calculation of such flows is quite a difficult problem in which the use of Prandtl mixing length and Prandtl-Kolmogorov turbulence-length-scale hypotheses are inadequate.

In the Power Profile concept two opposing jets meet on the rear side of the control surface before merging into the downstream direction. This sort of problem has been studied by Kind and Suthanthiran[49], who have developed some empirical relations for predicting the location where the two jets meet and then turn away from the wall. In their experiments they found that there was little loss in momentum in the mixing process, but that the merged or free jet has a rate of spread and turbulence level about three times as large as a conventional turbulent jet.

As expected, the position of the jet merger is half way between the two jet nozzles for equal values of jet momenta. As the momentum of the first jet is increased over that of the second, the merger position is moved toward the second jet. This is the type of phenomena desired for regulating the circulation about a Power Profile airfoil. However, Kind and Suthanthiran varied their momenta by varying the stagnation pressures of the two jets independently while both nozzle widths t were equal. In contrast, for Power Profiles the stagnation pressures of the two jets are equal, and the jet momenta are varied by changing the nozzle widths, t_ℓ and t_u. This difference is expected to be no problem to Power Profile operation.

Circulation-Control and Jet-Flap Experiments. Maurice Roy[32] reports briefly on a jet flap of the type shown by Figure 1e. Tests at ONERA have shown that such a flap is capable of high values of C_L, but even larger C_L values are possible when the lower jet flow is cut off. This is just what happens in a Power Profile flow when the control surface is deflected fully downward. In fact, with the lower jet shut off, the extended trailing edge shown in Figure 1e may be a disadvantage in obtaining the largest possible $C_{L_{max}}$, because the wall jet flow cannot turn around the trailing edge and travel forward on the lower surface.

Other French experiments with two jets at the rear of an airfoil are reported by Werlé[11]. This configuration, illustrated in Figure 3, was

suggested by Mr. Maurice Roy, Director of ONERA, and is essentially different from the Power Profile concept by the use of two different plenum pressures rather than nozzle widths to vary the two jet momenta. Kind and Maull[9] also used two different plenum pressures for some of their experiments. The Werlé configuration was subject to testing in a water-tunnel[11], used for its excellent flow-visualization capability. With C_μ = 0.3 for both the upper and the lower jets, the two jets merged smoothly along a horizontal line at the rear of the airfoil. This flow was in marked contrast to the separated and unsteady flow over the rear of the profile when there was no jet blowing. When the upper jet C_μ was increased to 0.6 and the lower jet C_μ decreased to 0.14, the merged jet stream was deflected downward at about 50° to the horizontal, and no flow separation was evident. No section C_L or other data are available, but this report is encouraging to the Power Profile concept.

Other jet flap experiments[32,35-47] are summarized in Table I below. The Jones[32] data is notable for its study of wall-jet development, but no lift data was recorded. Fink[35,36] shows an example of an unusual powered airfoil idea that did not work out very well. This is a good example of a flow too complex to be assessed by theoretical methods; hence, some general features of the flow were not predicted in advance of the experiments.

Kizilos, in Reference 37, presents some test data for his "VDT" airfoil which is illustrated in Table I. This airfoil has two trailing edge jets, but the airfoil is much thinner than the two-jet airfoil of Kind and Maull[9]. The data is rather disappointing, since it does not show a C_L with jet blowing of more than about 0.8 for $\alpha = 0°$; at $\alpha = 4°$, $C_L = 1.0$ is shown. It would be helpful to have a systematic set of curves showing C_L as a function of α and jet flap angle for each Mach number. The C_L available from VDT jet deflection and blowing is quite small at transonic speeds, and not much drag data is available.

The VDT airfoil geometry is significantly different from the Power Profile concept. For example, the VDT airfoil uses a biconvex control surface rather than a circular one, which was rejected because the jet could not be deflected sufficiently as the plenum to ambient pressure ratio became highly supersonic. The circular shape is much like that used on the Power Profile concept, which has not been configured for supersonic jet operation. In fact, as shown on Figure 59 of Reference 37, the pressure ratio for VDT jet detachment from the biconvex surface is greater than 2 so that the VDT jet is supersonic before the jet detachment arises. The mixture of the supersonic jet flow with the subsonic airfoil boundary layer is a difficult problem at best, so that the VDT jet detachment problem is not surprising. With some design changes the VDT airfoil might be able to avoid the jet detachment. Certainly, if one is to design a VDT airfoil for operation at $M_\infty < 1$, it would appear best to avoid supersonic flow difficulties as much as possible by keeping the jet speeds to no greater than low supersonic values.

The "TJ" airfoil is the second airfoil by Kizilos[38] shown on Table I. The test data for this airfoil is more encouraging since it shows good control of C_L in the transonic speed range. However, it may be possible to reduce drag through better shaping of the airfoil trailing edge region. Because of the geometric differences between the TJ airfoil and the Power Profile concept, the TJ data does not appear to be useful for Power Profile development efforts.

The circulation control airfoil data of Englar[39] is quite interesting, but suffers because almost all data runs were made at $\alpha = -1.2^\circ$ rather than 0° as was intended. The 30° jet flap configuration was the least effective of the three sections tested, possibly because of separated and unsteady flow conditions near the jet exit, as sketched in the Figure 9 given by Roy[31].

Alexander and Williams[40] have tested an airfoil and flap with jet BLC on a semispan aircraft model having an aspect ratio of 6. The two sets

of data each in the C_L and the α columns of Table I refer to two different values of flap deflection, $\delta_F = 90^\circ$ and 30°, respectively. At $\delta_F = 90^\circ$ a $C_L = 5.3$ is available for $C_\mu = 0.95$. For $C_\mu = 0.10$ the configuration has $C_L = 2.2$, which is larger than given by Englar[39], who used a thicker (15%), two-dimensional airfoil. The Alexander and Williams results are interesting because they show that it is possible to get large values of C_L on a section only 12 percent thick and a C_μ near 1.0, which is typical for aircraft takeoff conditions.

Even larger values of C_L at high C_μ were obtained by Malavard, Jousserandot, and Poisson-Quinton[41,42,43] using a configuration like that shown in Figure 1e. The larger of the two C_L values in Table I was obtained by blocking the flow out of the lower jet, so that only the upper jet was blowing. The 22.5 percent airfoil thickness was of some help in obtaining these large C_L values. A large variety of early French research on jet flap items has been reviewed by Poisson-Quinton and Lepage[1,44].

Related results were obtained by Kind and Maull[9] using a 20 percent elliptic airfoil section with a rounded trailing edge and a thin slot for blowing over the trailing edge. At $\alpha = 0^\circ$ and $C_\mu = 0.10$, they obtain $C_L = 1.9$, which is a little less than the $C_L = 2.5$ obtained by Malavard et al[41] under the same conditions.

Williams[3] using a 20 percent thick section obtained $C_L = 4.5$ at the above α and C_μ, $\alpha = 0^\circ$ and $C_\mu = 0.10$. The Williams' section was elliptic but modified by a 5.0 percent circular arc camber line. Furthermore, the Williams trailing edge radius was modified to 5.0 percent of the chord, whereas the Kind trailing edge was only 3.8 percent of the chord. Both the larger trailing edge and the camber of the Williams section would be expected to add to the C_L; so the larger C_L of the Williams section is not surprising. It is interesting that C_L for the Kind section goes to 3.2 as α goes to 15°, but the Williams section stalls with a decrease in C_L before α reaches as much as 5°. These observations seem to all be

consistent with each other and with what theory might predict. However, it is a little surprising that the Williams values of C_L are as large as reported; intuitively one might expect somewhat smaller C_L's. Here, it might be noted that the Williams C_L values were determined by static pressure readings on the floor and ceiling of the tunnel, including a 13 percent correction for the pressure footprint beyond the ends of the test section. Standard wind tunnel corrections have been applied to account for the tunnel blockage ratio $t/h = 0.08$, which is larger than for any of the other models shown in Table I. Recent experience at Douglas Aircraft Company[45] has shown that such standard tunnel corrections are often in error, so the results should be viewed with caution. A better procedure for finding corrections is to use the Neumann potential flow method or the Douglas non-linear jet-flap potential flow method for calculating the model flow fields both in the tunnel test section and in free air; this is done in Reference 45. The Williams result of $C_{L_{max}} = 6.3$ at $C_\mu = 0.23$ is near the maximum, $2\pi(1 + t/c)$, predicted by non-linear theory for the two stagnation points brought together on the bottom surface of the airfoil.

Extremely large values of C_L, such as the 15.8 obtained by Malavard et al[41], may not be of great interest because of at least two practical difficulties in applying such a flow to a wing of finite aspect ratio. Such C_L values produce very large values of induced drag; at the same time the large values of U_J/U_∞ required to generate the large C_L values results in a very poor propulsive efficiency. Because of this high drag and low propulsive efficiency, C_L values in the neighborhood of 6 to 9 may be about the upper limit for application to STOL aircraft at the moment of takeoff or landing.

The work in References 3, 9, and 40 to 44 illustrate that C_L values up to 6 can be obtained for C_μ values up to about 0.23; what one would like for applications is more detailed experimental information on such airfoils. Re_c in these tests did not exceed 0.9×10^6; tests at larger Reynolds numbers would be desirable. Further testing of the drag and

control aspects of such airfoils at more moderate or cruising values of C_L are needed. Transonic testing is needed. In general, a full development program on powered airfoils should be undertaken.

Discussion of the work of Grahame and Headley[46] and of Peake, Yoshihara, Zonars, and Carter[47] has been saved until last because of the special nature of these transonic tests. The Reynolds numbers and Mach numbers of these tests are larger than most of the other work reported in Table I. The Peake tests are notable for the values of Re_c, which are about the same as full-scale flight, and much larger than the usual wind tunnel test values. The airfoils for these two tests have much in common, the principal difference being the thickness-to-chord ratio, which is 6.6 percent for the Grahame section and 10.0 percent for the Peake section. Both airfoils have a trailing edge deflected downward in the manner of a Whitcomb airfoil; this feature is more pronounced on the thicker Peake section than on the Graname section. Finally, both airfoils have a trailing edge jet flap with several configurations having the jet nozzle deflected downward at various angles between 0° and 90°.

These two tests showed the same general trends of an increase in lift and buffet onset boundary with jet flap flow. The airfoil shock waves were moved downstream with jet blowing, and high levels of thrust recovery were obtained. The reader is referred to References 46 and 47 for further detail.

6. DEVELOPMENT OF A POWER PROFILE CONFIGURATION

The objective of this section is to show the theoretical development of a Power Profile shape, including the jet control system, suitable for use as a wind tunnel model. At the start of this study the author suggested that a symmetric airfoil (zero camber) be used for initial tunnel tests of the Power Profile concept; but, as the study advanced, the author developed the procedures needed to design an airfoil with moderate camber. The

inclusion of camber has made the design effort more complex, but the resulting airfoil should be better suited both to high lift and to cruising flight conditions than would be a zero camber airfoil. At the start of this study the author put forth the idea of using free-streamline shapes as a starting point for the Power Profile concept. At that time the only free-streamline shapes which had been developed and could be applied were those of Pierce, Hess, and Smith[12]. These all were zero-camber sections; hence, the decision to use symmetric sections was appealing. Since that time, the powerful inverse design technique of James[14] has become available; and, with this method, shapes such as shown in Figure 10 were developed.

With the James method available, the question arose as to how much camber and thickness should be designed into the test airfoil. As explained in Section 2, the use of free-streamline shapes enables one to have a larger airfoil thickness than otherwise possible for a given value of superstream velocity. Hence the airfoil should be thick, and t/c = 22.5 percent was chosen. This thickness results in a slightly lower value of maximum surface velocity than is obtained on airfoils such as the NACA 64_2A015 or the 65_2-015 sections at zero lift, which have a t/c = 15.0 percent. The 22.5 percent is somewhat thicker than the Williams[3] and the Kind and Maull[9] sections, which had t/c = 20.0 percent. It is clear that this decision is a compromise between the advantages of high structural strength and high lift, which come with thicker sections, and a high critical Mach number[13], which comes with a thinner section. Another important reason for choosing this thick section is that the problem of leading edge separation is minimized.

The selection of the amount of camber was a compromise between the conflicting requirements of high lift on the one hand and good cruising characteristics on the other. As stated above, it also was desired to keep the camber small so as to avoid the probable difficulty of mixing high camber with the Power Profile jet concept in the first design study.

With these considerations, a design C_L of 0.50 was chosen; this constraint indirectly specified the camber.

The airfoil shape to be used also was influenced by its suitability for the two jets that characterize the Power Profile concept. This may be illustrated through the use of Case 9 shown on Figure 10. On this shape in low speed flow the adverse pressure gradients start near 96 percent chord on the upper surface and 95 percent chord on the lower surface. Hence, the two control jets should be placed near these two locations so as to maintain unseparated flow around the trailing edge. These two locations are apart by a distance s_j = 11.3 percent in terms of chord length. Therefore, s_j is a measure of the distance the two jets must travel before merging together, and it is desirable to minimize s_j so that the jet energy required to overcome separation is minmized.

The James design method as used here is a technique for incompressible flow. The incompressible results may be corrected for compressibility by using the Karman-Tsien rule[13], which gives results reasonably well up to and somewhat past the critical Mach number. More advanced analytical techniques are required for airfoil design at greater speeds.

In summary, the three goals of the airfoil shaping study are t/c = 0.225, $C_{L_{design}}$ = 0.50, and that s_j should be as small as possible. While the airfoil boundary layer character has not been mentioned explicitly here, its influence has not been overlooked. In general, the boundary layer is thin enough so that the pressure distributions such as given in Figure 10 by the James method are close to that on the airfoil with the boundary layer effect added. Of greater importance are the changes in this pressure distribution that come from angle of attack changes. The boundary layer displacement thickness will make the zero pressure gradients in Figure 10 slightly favorable, but these

gradients are easily overpowered by the effects of angle of attack. The boundary layers will be able to withstand some adverse gradient without separation; this subject is discussed in depth by Smith[18]. Hence, the above three goals are compatible with such boundary layer considerations.

Shaping of the Airfoil by the James Design Method. In meeting the above design goals, eighteen separate runs of the James program[14] were used. The results of runs 7 and 9 are shown in Figure 10. The remaining runs were used to vary the input parameters, such as shown in Figure 11, in a systematic manner. The final run resulted in the shape shown in Figure 12, for which $t/c = 0.2245$, $C_L = 0.482$, and $s_j = 0.089$. The velocity ratio on the lower surface is $V_l = 1.110$. On the upper surface it is $V_u = 1.309$. The start of the adverse pressure gradient on the upper surface is at 98.6 percent chord; on the lower surface it is 98.2 percent. These are further aft than those of Case 9 on Figure 10, and s_j is smaller than for Case 9.

Jet Locations and Control Surface Shaping. The design airfoil shape illustrated in Figure 12 is shown in Figure 13 with a trailing edge modification for two jets and a control surface. The jet exit planes on Figure 13 were located just ahead of the adverse pressure gradients shown in Figure 12 so that the jets could be used to overcome these gradients. Then each of the upper and lower surface trailing edge lips was designed with a local thickness equal to 12 percent of the distance from the trailing edge apex. The control surface was then contoured so that the slot or nozzle passageways became narrower in the streamline direction and so as to insure that the jets would experience a rapid acceleration just ahead of the jet exit planes. At each of the two exit planes the slot width was made equal to 0.50 percent chord. The remainder of the control surface was then drawn with its "trailing edge" or rear stagnation point as far forward as practical so that the streamline running off each of the other two trailing edges might follow as closely as practical to the aft end contour of the airfoil, as shown on

Figure 12. Of course, these two streamlines cannot meet at a rear stagnation point, as in Figure 12. The flow field was then studied by using the Douglas Neumann inviscid flow program to calculate the pressure distribution, which gave results somewhat different than shown on Figure 13. Then the control surface was reshaped slightly to that form shown in Figure 13, and the Neumann program was run again, with the results as shown in Figure 13.

Since the Neumann program requires that the jet plenum pressure be equal to the free stream total pressure, and since the method does not account for the viscous effects which may be quite important, the pressure distribution shown on Figure 13 is of value mainly in the inside portion of the airfoil. Whether or not the slight adverse gradients shown on Figure 13 on the upper and lower external surfaces are real cannot be determined by present methods, and experiments should help clarify this point. The jet entrainment effect will tend to make these gradients favorable. For the Neumann calculation the three rear stagnation points were placed at the two trailing edges and on the control surface at $y = 0$.

The Douglas Non-Linear "Jet Flap" Potential Flow Method currently under development has been used to study the effect of jets on the flow about the airfoil given in Figure 12. The jet with $C_\mu = 0.02$ was first placed at $y = 0$ on the trailing edge and pointed 5° downward from the horizontal. This resulted in a very small change from the pressure distribution shown in Figure 12. However, when the jet strength was increased to $C_\mu = 0.5$ with the jet deflected downward at 60° and located at $x/c = 0.9800$, $y/c = -0.0376$, the pressure distribution changed to that shown on Figure 14 with $C_L = 5.67$. When C_μ was reduced to 0 but with the rear stagnation point retained at $x/c = 0.9800$, C_L was reduced to 2.88. This shows the striking difference that the jet flap effect makes on the pressure distribution. As discussed in Section 2, at high lift conditions there are adverse pressure gradients on the upper surface. The

gradients shown for the forward part of the airfoil on Figure 14 have been checked against the Stratford separation criterion[10], and the boundary layers are not close to separation. It is expected that the greater pressure rise at the rear for $C_\mu = 0.50$ will be handled adequately by the greater C_μ.

In spite of the recent development of powerful methods for the calculation of both the viscous and the inviscid portions of the airfoil flow fields[14, 15, 17, 19, 20, 28, 30] these methods are not really adequate to predict the mixing of the Power Profile wall jets, boundary layers, the jet merging region, and the jet downstream of the trailing edge. Although the general features of the flow field are known from elementary principles, important details such as mixing and entrainment cannot be adequately calculated. The details of the flow field involve turbulence processes which are not fully understood. Hence, the only way of determining the overall characteristics of such flow fields with accuracy is through experimental work.

Control Surface Travel. Figure 15 illustrates a simple mechanical method for rotating the control surface given in Figure 13. In order to control the strengths and thicknesses t_ℓ and t_u of the two jets, it is desirable from an inertia point of view and also from a jet-nozzle shaping point of view to have point A of the surface travel along the line BC, which is approximately perpendicular to the jet stream. At the same time, like reasoning makes it desirable for point D to travel along the line EF. Thus t_u is equal to AC and t_ℓ is equal to DF.

To accomplish this, an obvious solution is to pivot the entire surface about point G, to the right, which was determined by the requirements that AG be perpendicular to BC and that DG be perpendicular to EF. This makes good mechanical sense, but is poor aerodynamically. A better aerodynamic choice for a surface pivot point would be H or I; then the mechanical supports would not appreciably interfer with the aerodynamics.

However, H and I are both very poor mechanical choices because such centers would not move point A along or even close to BC, nor would point D move along EF. A solution to this problem is to use links JK and LM, fixed but free to rotate about points J and L and attached to but free to rotate on the control surface at points K and M. Thus points K and M will move in circular arcs about J and L, respectively. Since the extensions of lines JK and LM intersect at G, the effective center for small control surface rotations is point G. Points A and D will deviate only a very small amount from the lines BC and EF, and the links JK and LM are away from critical flow regions. Thus, JKML is a four-bar linkage which constrains the surface motion appropriately.

Mechanical actuation of the control surface can be accomplished through an actuator attached to any point such as N which is not close to G. The surface at full deflection is shown in Figure 15 by the dotted lines.

Another method of constraining the surface motion would be to use tracks.

For experimental purposes it is useful to be able to vary the sum of the two nozzle widths, $(t_\ell + t_u)$. This can be done by building several different control surfaces. A better method might be to build only one surface having a split along the line OP. Then various shims could be placed along OP, which would result in new values of $(t_\ell + t_u)$.

Wall Jet Calculations. As shown in Figure 13, the jet flow over the control surface and downstream of the jet nozzles has a steep adverse pressure gradient which, except for the action of the jet, would lead to boundary layer separation. In order to study this problem further, the integral method of Gartshore and Newman[28] has been used to calculate some sample wall-jet and boundary-layer interactions, as shown on Figures 16 and 17. In both cases shown on the figures, the jet velocity

U_J is assumed to be $2U_\infty$, and the boundary layer edge velocity U_e is assumed to go from $1.3U_\infty$ linearly to zero in a distance of 0.05 chord length, which is about equal to the distance from the Power Profile jet exit to the rear stagnation point. In both cases the boundary layer before jet mixing is assumed to have a thickness of 2.0 percent chord, and the profile is of the 1/7 power type. Here it is noted that the Gartshore Newman method neglects to account for any pressure gradients normal to the wall.

The only difference between Case 1 and Case 2 is that the nozzle width t_u is only 0.0015 chord in Case 1 as compared to 0.0030 chord in Case 2. According to the table, for Case 1 the jet momentum excess thickness, defined by

$$\theta_J = \left(\frac{U_J}{U_e}\right)\left(\frac{U_J}{U_e} - 1\right) t_u \tag{4}$$

is smaller than $\theta_{B.L.}$, the boundary momentum thickness at $x = 0$, just before mixing with the jet. On the other hand, Figure 17 shows for Case 2 that $\theta_J > \theta_{B.L.}$.

The Gartshore-Newman method assumes that the jet and the boundary layer mix instantly at $x = 0$ and that thereafter the combined velocity profile $u(y)$ is given by relations in the form

$$\frac{u}{U_m} = \left(\frac{y}{y_m}\right)^n \qquad 0 \le y \le y_m \tag{5}$$

$$\frac{u}{U_m - U_e} = \frac{U_e}{U_m - U_e} + e^{-k\left(\frac{y - y_m}{L_o}\right)^2} \qquad y \ge y_m \tag{6}$$

where $k = \log_e 2$. Hence, y_m is the thickness from the wall to the maximum velocity U_m. L_o is the distance from y_m to $y = y_2$ where u is half way between U_m and U_e. That is,

$$y_2 = y_m + L_o \tag{7}$$

This form of velocity profile is illustrated in Figure 16.

The form of the velocity profile at x = 0 and for $\theta_J > \theta_{B.L.}$ is determined by setting $y_m = t_u/3$ and n = 1/11 or 1/7 depending on whether U_J is greater than or less than $2U_e$, respectively. Then momentum and continuity relations are used to determine U_m and L_o. If it turns out that this gives $U_m > U_J$, U_m is set equal to U_J and L_o is determined by the momentum relation. For cases such as Case 1 where $\theta_J < \theta_{B.L.}$, L_o is taken to be zero and $U_m = U_e$ so that only equation 5 is required to determine u. Then n = 1/7 and y_m is determined by the momentum relation, which is just $y_m = \frac{72}{7} (\theta_{B.L.} - \theta_J)$. As stated by Gartshore and Newman, such a simple velocity profile becomes increasingly suspect as $\theta_{B.L.}/\theta_J$ increases above unity.

For x > 0, integral relations are used to determine the profile parameters y_m, L_o, U_m, and n. Boundary layer separation has been correlated with n as occurring whenever n reaches 0.50.

Figure 17 shows dramatic differences between Case 1 and Case 2. Case 1 results in a boundary layer separation at x/c = 0.012. Case 2 does not separate even though it is calculated to x/c = 0.05, where $U_e = 0$. The thickness parameters y_2 and y_m are much larger in Case 1 than in Case 2. Hence, we see that the wall jet results depend markedly on the parameter $\theta_J/\theta_{B.L.}$. For this reason, and because the calculations do not account for many factors, experiments are needed to determine the minimum values of $\theta_J/\theta_{B.L.}$ needed to avoid separation on Power Profile shapes. Yet this rough calculation indicates that moderate values of C_μ will prevent separation.

Although the method of Gartshore and Newman appears to be as valid as any presently-available method, it does not provide answers to all the complex flow phenomena of concern in Power Profile design and analysis.

One would like to account for the pressure gradient normal to the wall, and to gain a better understanding of the mixing region between the jet and the boundary layer. Because these questions and many others can be raised about the applicability of wall jet calculations, experimental results are needed for full development of Power Profile configurations.

Power Profile Performance. In the above wall-jet discussion, the parameter $\theta_J/\theta_{B.L.}$ is of central importance in avoiding separation, which is essential to satisfactory performance. In this discussion we will see now how this parameter plays a role in Power Profile design for both cruise and high-lift conditions.

For the shape shown in Figures 12, 13, and 15 the superstream velocity ratios V_ℓ and V_u on the lower and supper surfaces, respectively, are 1.100 and 1.308 as shown in Table II below. For Re_c equal to about

TABLE II

Power Profile Jet Performance Parameters at Cruise, $C_L = 0.5$

Parameter	Case A	Case B
V_ℓ	1.100	1.100
V_u	1.308	1.308
$(\theta_{B.L.}/c)_\ell$	0.0020	0.0020
$(\theta_{B.L.}/c)_u$	0.0020	0.0020
$(\theta_J/c)_\ell$	0.0026	0.0026
$(\theta_J/c)_u$	0.0026	0.0026
U_{J_∞}/U_∞	1.50	2.00
$(U_J/U_\infty)_\ell$	1.57	2.05
$(U_J/U_\infty)_u$	1.72	2.17
t_ℓ/c	0.0043	0.0016
t_u/c	0.0063	0.0024
C_{μ_ℓ}	0.020	0.013
C_{μ_u}	0.033	0.021
$C_\mu = C_{\mu_\ell} + C_{\mu_u}$	0.053	0.034
C_μ'	0.021	0.018

3×10^6, the ratio $\theta_{B.L.}/c$ will be about 0.0020 on both the upper and lower surfaces. Suppose that such a boundary layer requires that the jets each have a θ_J/c equal to 0.0026 to avoid separation. This requirement then will determine the blowing required to avoid separation.

For good propulsive efficiency in cruise the ratio U_{J_∞}/U_∞ should be on the order of 1.50 to 2.00 where U_{J_∞} is defined as the speed that the jet would obtain if it were expanded isentropically form the jet plenum pressure to the free stream pressure p_∞.

Thus, in the incompressible approximation, the jet plenum pressure is $p_\infty + q_\infty (U_{J_\infty}/U_\infty)^2$, where q_∞ is the free-stream dynamic pressure. If we take $(U_{J_\infty}/U_\infty) = 1.50$, as in Case A in Table II, then the (U_J/U_∞) for the upper and lower surfaces are determined as given in the table. Then t_ℓ/c and t_u/c must be 0.0043 and 0.0063 respectively, so as to avoid separation. These parameters determine C_{μ_ℓ} and C_{μ_u} as shown. Thus, $C_\mu = 0.053$ to avoid separation for $U_{J_\infty}/U_\infty = 1.50$ and the assumed values of θ_J.

In Case B, where $U_{J_\infty}/U_\infty = 2.00$, C_μ needs to be only 0.034 to avoid separation. Thus, the selection of U_{J_∞}/U_∞ determines both the slot widths, t_ℓ and t_u, and C_μ. However, C_μ', defined by equation 3, is about the same for both cases.

The above cases were calculated using incompressible flow relations. For an aircraft at high subsonic cruise or greater speeds, compressibility corrections must be made, and the flow analysis is much more complex. Compressible phenomena will be important for the design to specific values of parameters such as U_{J_∞}/U_∞.

The parameters in Table II are expected to be conservative; perhaps θ_J need be only 0.0020 or less in order to avoid separation. Then the required t_ℓ, t_u, and C_μ will be smaller. This shows the importance of and experimental program to establish such operating parameters.

These parameters also affect the operation of the Power Profile at high lift conditions, as shown below in Table III. For this table, the

TABLE III

Power Profile Jet Performance Parameters at High Lift, $C_L = 6.0$

Parameter	Case A	Case B
t_ℓ/c	0	0
t_u/c	0.0106	0.0040
C_{μ_ℓ}	0	0
C_{μ_u}	0.25	0.25
(U_J/U_∞)	4.14	6.00

lower jets are closed, so that $t_\ell = 0$, and t_u is opened up so that it is equal to the sum $(t_\ell + t_u)$ given in Table II. Then, assuming that $C_\mu = 0.25$ will given $C_L = 6.0$, we find the values of (U_J/U_∞) required. Thus the plenum pressure must be adjusted to attain these values of U_J; however, the plenum pressure may not be any larger than required for Table II, since U_∞ at $C_L = 6.0$ will be much smaller than that at $C_L = 0.50$ or cruise conditions.

The above was based on $C_\mu = 0.25$, since 0.25 is close to Williams experimental value[3] of 0.23 for a like value of C_L, as discussed in Section 5. The actual values of C_μ required to obtain large values of lift coefficient need to be checked experimentally before many further applications of Power Profile performance can be established.

Drag at Cruise Conditions. Very little has been said about drag because of the implicit assumption that drag will be low if separation is avoided. Because of the integrated nature of the Power Profile drag and propulsive systems, the drag cannot be separated from its effect on propulsive efficiency. This is a complex subject, as Stratford[4,5] has pointed out, but overall gains are expected[4,5]. Because of the complexity of this subject, experimental programs are needed to fully assess this potential for drag savings and propulsive benefits.

7. CONCLUDING STATEMENTS

A review has been made of the literature and methods applicable to the Power Profile concept. Both theoretical methods and experimental data on circulation-controlled airfoils have been included. The experimental data has served as a guide to the fact that C_L values in the neighborhood of 6.0 are attainable for values of C_μ near 0.25. This assumed that the airfoil has a thickness ratio of 0.20 or somewhat larger. With this in mind an airfoil shape with a thickness ratio of 0.225 has been designed using the theoretical design method of James[14]. The James method was used to give the airfoil a constant pressure shape over most of the upper and lower surfaces for a cruise C_L of 0.5. The potential flow method of Hess and Smith[15] was used as an aid to designing the aft portion of the airfoil, and the Gartshore-Newman method[28] was used to obtain a very rough and probably conservative estimate of the jet power required to avoid separation.

It is concluded that this airfoil shape, as shown in Figures 12, 13, and 15, should be tunnel tested to determine the overall level of airfoil performance. Of special interest is the amount of jet momentum required to avoid separation under cruise conditions, and the effect of the integration of the airfoil and propulsive systems in minimizing drag for a given power input. The second area of interest is in how much jet momentum is required to produce C_L values in the neighborhood of 6.0, and in the sensitivity of C_L to control surface deflections. Because of the complexity of the jet, boundary layer, and potential flow interactions, no presently available theoretical methods are adequate to predict Power Profile performance completely, and hence an experimental program is required.

Assuming that subsonic tests are promising, one would need transonic testing to evaluate the unique characteristics of the concept at transonic speeds. This might be done using an airfoil having a thickness ratio of, say, 0.14. One should then investigate as to what extent the Power Profile concept might improve critical Mach number and delay the transonic drag and buffeting as compared to a conventional transonic section having the same thickness ratio.

8. REFERENCES

1. Poisson-Quinton, Ph., and Lepage, L., "French Research on Control of Boundary Layer and Circulation", as found in the book Boundary Layer and Flow Control by G. V. Lachmann, Pergamon Press, 1961.

2. Attinello, J. S., "Design and Engineering Features of Flap Blowing Installations", as found in the book Boundary Layer and Flow Control by G. V. Lachmann, Pergamon Press, 1961.

3. Williams, R. M., and Howe, H. J., "Two-Dimensional Subsonic Wind Tunnel Tests on a 20 Percent Thick, 5 Percent Cambered Circulation Control Airfoil", AD 877-764, NSRDC Technical Note AL-176, August 1970.

4. Stratford, B. S., "Mixing and the Jet Flap", The Aeronautical Quarterly, Volume 7, pp. 85-105, May 1956.

5. Stratford, B. S., "A Further Discussion on Mixing and the Jet Flap", The Aeronautical Quarterly, Volume 7, pp. 169-183, August 1956.

6. Brown, D. A., "Public Acceptance Key to STOL", Aviation Week and Space Technology, see p. 22, March 6, 1972.

7. Dorsch, R. G., Krejsa, E. H., and Olsen, W. A., "Blown Flap Noise Research", NASA TM-X-67850, June 1971.

8. von der Decken, J., "Aerodynamics of Pneumatic High-Lift Devices", AGARD Lecture Series No. 43, Assessment of Lift Augmentation Devices.

9. Kind, R. J., and Maull, D. J., "An Experimental Investigation of a Low-Speed Circulation-Controlled Aerofoil", The Aeronautical Quarterly, Volume 19, pp. 170-182, 1968.

10. Stratford, B. S., "The Prediction of Separation of the Turbulent Boundary Layer", Journal of Fluid Mechanics, Volume 5, January 1959, pp. 1-16.

11. Werlé, H., "Investigations of Blowing in a Water Tunnel by Flow Visualization", NASA Technical Translation TT F-13, 742, August 1971, pp. 32, 33.

12. Pierce, J., Hess, J. L., and Smith, A. M. O., "Velocity Distributions and Shapes for Free-Streamline Bodies Having Wedge-Shaped Noses", Douglas Aircraft Company Report ES-29123, August 1958.

13. Abbott, I. H., and Von Doenhoff, A. E., "Theory of Wing Sections", Dover Publications, 1959.

14. James, R. M., "A New Look at Two-Dimensional Incompressible Airfoil Theory", Douglas Aircraft Company Report MDC-J0918/01, May 1971.

15. Hess, J. L., and Smith, A. M. O., "Calculation of Potential Flow About Arbitrary Bodies", Progress in Aeronautical Sciences, Volume 8, Pergamon Press, New York, 1966.

16. Schlichting, H., "Boundary Layer Theory", McGraw-Hill, New York, 1968.

17. Cebeci, T., Smith, A. M. O., and Wang, L. C., "A Finite-Difference Method for Calculating Compressible Laminar and Turbulent Boundary Layers", Douglas Aircraft Company Report DAC-67131, March 1969.

18. Smith, A. M. O., "Aerodynamics of High-Lift Airfoil Systems", Presented at the AGARD Fluid Dynamics of Aircraft Stalling Meeting in Lisbon, Portugal, April 1972.

19. Cebeci, T., Mosinskis, G. J., and Smith, A. M. O., "Calculation of Separation Points in Incompressible Turbulent Flows", Journal of Aircraft, Volume 9, pp. 618-624, September 1972.

20. Cebeci, T., Mosinskis, G. J., and Smith, A. M. O., "Calculation of Viscous Drag and Turbulent Boundary-Layer Separation of Two-Dimensional and Axisymmetric Bodies in Incompressible Flows", Douglas Aircraft Company Report MDC-J0973/01, November 1970.

21. Glauert, M. B., "The Wall Jet", Journal of Fluid Mechanics, Volume 1, pp. 625-643, 1956.

22. Kruka, V., and Eskinazi, S., "The Wall Jet in a Moving Stream", Journal of Fluid Mechanics, Volume 20, pp. 555-579, 1964.

23. Abramovich, G. N., "The Theory of Turbulent Jets", The M.I.T. Press, 1963.

24. Harris, G. L., "The Turbulent Wall Jet in a Moving Stream", Proceedings of Specialist Meeting Sponsored by AGARD Fluid Dynamics Panel, May 1965.

25. Newman, B. G., "The Prediction of Turbulent Jets and Wall Jets", Canadian Aeronautics and Space Journal, Volume 15, pp. 288-305, 1969.

26. Gartshore, I. S., "Prediction of the Blowing Required to Suppress Separation from High-Lift Aerofoils", Canadian Aeronautics and Space Institute Transactions, Volume 4, pp. 34-46, 1971.

27. Thomas, F., "Investigation of the Increase of Lift of Lifting Wings by Means of B. L. Control by Blowing", Translated from the original German, Z. Flugwiss, 10, 1962, Heft 2, pp. 46-65.

28. Gartshore, I. S., and Newman, B. G., "The Turbulent Wall Jet in an Arbitrary Pressure Gradient", The Aeronautical Quarterly, pp. 25-56, February 1959.

29. Kelly, M. W., "Analysis of Some Parameters Used in Correlating Blowing Type Boundary Layer Control Data", NACA RM A56F12, 1956.

30. Ambrosiani, J. P., and Ness, N., "Analysis of a Circulation Controlled Elliptical Airfoil", West Virginia University Aerospace Engineering Report TR-30, April 1971.

31. Maskell, E. C., and Gates, S. B., "Preliminary Analysis for a Jet-Flap System in Two-Dimensional Inviscid Flow", R. A. E. Aero Report 2552, June, 1955.

32. Jones, D. G., "The Performance of Circulation-Controlled Airfoils", Cambridge University Thesis", August 1970.

33. Kacker, S. C., and Whitelow, J. H., "Some Properties of the Two-Dimensional Turbulent Wall Jet in a Moving Stream", Journal of Applied Mechanics, Volume 35, pp. 641-651, December 1968.

34. Kacker, S. C., and Whitelow, J. H., "The Turbulence Characteristics of Two-Dimensional Wall-Jet and Wall-Wake Flows", Journal of Applied Mechanics, Volume 38, pp. 239-252, March 1971.

35. Fink, M. R., Stoeffler, R. C., "Preliminary Investigation of the Counter-Flow Jet Flap", NASC Report dated March 1970.

36. Fink, M. R., "Wind Tunnel Investigation of a Counter-Flow Jet Flap", NASC Report dated June 1970.

37. Kizilos, A. P., and Rose, R. E., "Experimental Investigations of Flight Control Surfaces Using Modified Air Jets", Honeywell Document No. 12055-FR1, November 1969.

38. Kizilos, A. P., Kizilos, B. M., and Smith, G. A., "Study of Blowing Transverse Jets from Airfoils for Flight Control Applications in the Mach Number Range 0.2 to 3.0", Honeywell Document No. 12146-FR, November 1970.

39. Englar, R. J., "Two-Dimensional Transonic Wind Tunnel Test of Three 15-Percent Thick Circulation Control Airfoils", NSRDC Technical Note AL-182, December 1970.

40. Alexander, A. J., and Williams, J., "Wind Tunnel Experiments on a Rectangular-Wing Jet-Flap Model of Aspect Ratio 6", Aeronautical Research Council R&M 3329, 1964.

41. Malavard, L., Jousserandot, P., and Poisson-Quinton, P., "Jet Induced Circulation Control", Parts I and II, Aero Digest, September, October, November 1956.

42. Poisson-Quinton, Ph., and Jousserandot, P., "Hypersustentation et Pilotage des Avions Par Controle de Circulation", Association Technique Maritime et Aëronautique, Session 1955.

43. Malavard, L., Poisson-Quinton, P., and Jousserandot, P., "Recherches Theoriques et Experimentales sur le Controle de Circulation par Soufflage Appliqué aux Ailes D'Avions", ONERA Technical Note No. 37, 1956.

44. Poisson-Quinton, P., "Some Physical Aspects of Blowing on Aircraft Wings", English translation taken from "Technique et Science Aeronautiques", No. 4, 1956.

45. Wasson, N. F., and Lopez, M. L., "An Analysis of Two-Dimensional Wind Tunnel Corrections", Douglas Aircraft Company Report MDC-J5036, in publication.

46. Grahame, W. E., and Headley, J. W., "Jet-Flap Investigation at Transonic Speeds", Report AFFDL-TR-69-117, February 1970.

47. Peake, D. J., Yoshihara, H., Zonars, D., and Carter, W., "The Transonic Performance of Two-Dimensional, Jet-Flapped Aerofoils at High Reynolds Numbers", National Research Council of Canada, report presented at Gottingen, German, 26-28 April 1971.

48. Goradia, S. H., and Colwell, G. T., "Parametric Study of a Two-Dimensional Turbulent Wall Jet in a Moving Stream with Arbitrary Pressure Gradient", AIAA Journal, Volume 9, pp. 2156-2165, November 1971.

49. Kind, R. J., and Suthanthiran, K., "The Interaction of Two Opposing Plane Turbulent Wall Jets", AIAA Paper No. 72-211, January 1972.

TABLE I

LIST OF AIRFOIL EXPERIMENTAL CONDITIONS AND COMMENTS

Report	t/c	t_e/c	C_L	C_μ	U_j/U_∞	α Degrees	M_∞	$Re_c \times 10^{-6}$	t/h	Jet Description	Comments
Fink[35,36] 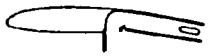	0.12	--	2.15 2.75 3.50	0.48 1.10 1.67	--	10	0.11	0.9	--	Counter flow jet flap	Lift augmentation was poor because of jet flap exhaust flow retrogestation at the trailing edge, producing a negative contribution to the airfoil circulation. The airfoil development has been stopped.
Kuzlos[37] VDT 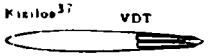	0.102	0.00114	0.80	0.053	0-5	0	0.2-0.1	1.0-3.5	0.055	Two trailing edge jets	Airfoil well developed for control purposes but is not suited for getting a large $C_{L_{max}}$. Low drag levels for cruising flight may not be obtainable.
Kuzlos[38] TJ 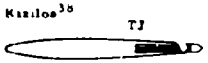	0.102	0.00114 0.0023	1.50	0.12	--	2	0.2-3.0	3.0-4.0	0.075	Two trailing edge jets	
Englar[39] 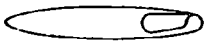	0.15	0.00125	1.75	0.06	0-10	-1.2	0.3-0.9	1.4-2.5	0.075	Wall jet at x/c = 0.924 and 0.960 Jet flap at x/c = 0.98	Almost all tests were conducted at α = -1.2° so that results are of limited value - $C_{L_{max}}$ is low.
Jones[32] 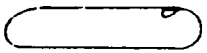	0.20	0.00245	--	--	2-4	--	0.016-0.033	0.42-0.88	0.136	Wall jet at x/c = 0.68 and 0.90	Wall jet development on flat and curved surfaces is shown.
Alexander and Williams[40] 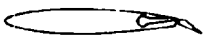	0.12	0.0040	1.4, 1.2 2.2, 1.6 3.8, 2.2 5.3, 2.9 7.5, 4.5	0 0.10 0.40 0.95 2.3	0-16	10, 11 4, 9 0, 9 1, 11 5, 14	0.05-1.0	0.5-1.0	0.022	Airfoil and flap with jet BLC	Three-dimensional model, AR = 6. C_L's are given for flap deflections of both 90° and 30°, respectively.
Malavard, Jousserandot and Poisson-Quinton[41,42,43] 	0.225	0.005	0.7, 0.7 2.5, 2.8 3.8, 3.4 7.3, 5.8 15.8, 11.8	0 0.1 0.5 1.0 4.0	0-20	0 0 0 0 0	0.02-0.10	0.12-0.66	--	Two trailing-edge jets, like Figure 1e.	Early French research. Larger C_L's attained using top jet only.
Kind and Maull[9] 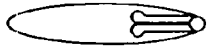	0.20	0.00055 0.0020	2.4 3.2 1.9	0.05 0.10 0.10	0-7	15 15 0	0.09	0.75	0.061	Two trailing-edge jets, much like Power Profiles.	Jet strength varied by changing plenum pressure, in general different for each jet. C_L's shown are using top jet only.
Williams[1] 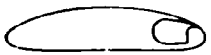	0.20	0.00125	2.8 4.5 6.3	0.04 0.10 0.23	0-10	0 0 0	0.12-0.19	0.56-0.89	0.080	Wall jet at x/c = 0.973	$C_{L_{max}}$ of 6.3 is large. This is a good example of an elliptical airfoil with blowing.
Grahame and Headley[46] 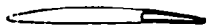	0.066	0.0020	1.51	0.029	1.05-1.40	11	0.70-0.95	2.5-5.5	0.014	Trailing edge jet flap	Jet flap improves the buffet boundary.
Peake, Yoshihara, Zonars, and Carter[47] 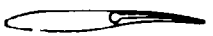	0.10	0.0030	1.31* 1.75*	0 0.02	0-2	6 6	0.7-1.0	11.0-40.0	0.025	"Whitcomb" type with trailing edge jet flap	Quite useful transonic test. Reynolds number is large.

*Value uncertain - see text.

FIGURE 1

SOME KEY FEATURES OF CIRCULATION CONTROL AND JET FLAP SYSTEMS

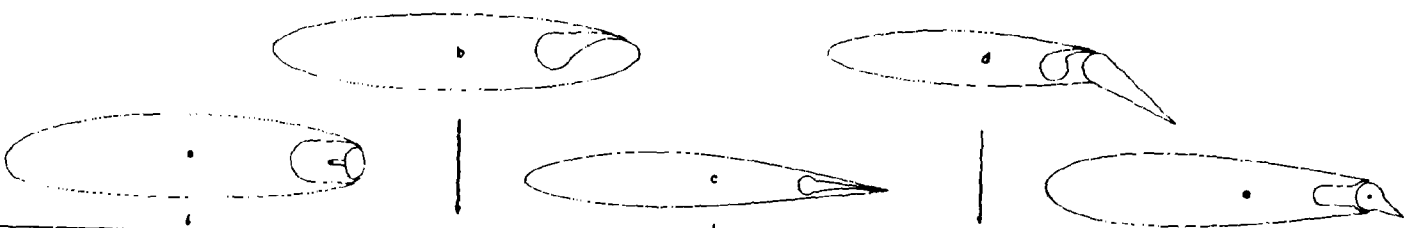

PROFILE TYPE	POWER PROFILE	SIMPLE SHAPE WITH CIRCULATION CONTROL	AIRFOIL WITH A PURE JET FLAP	CONVENTIONAL AIRFOIL AND FLAP WITH JET B L C	EARLY FRENCH JET FLAP
C_μ Range -typical	0.01 to 1.0	0.01 to 1.0	0.03 to 1.0	0 to 0.05 (0.03 to 1.0)*	0.01 to 1.0
$C_{L_{max}}$ for above C_μ range	1.5 to 6.0	1.5 to 6.0	1.6 to 4.0	2.2 to 4.0 (2.5 to 7.0)*	1.5 to 5.0
Is airfoil operable efficiently with no blowing?	No	No	Yes	Yes	No
Control method	Control surface deflections plus variable C_μ: motion small	Variable C_μ - this also affects the jet thrust	Jet deflection possible but difficult	Flap deflection	Control surface deflections plus variable C_μ: motion large
Control system inertia	Low	Low	Low	High-large surface	Moderate
Jet nozzle width	Variable with control surface deflection	Fixed	Fixed	Fixed	Fixed
Do adverse pressure gradients exist just upstream of jets?	No at design condition; yes at large angles of attack	On lower surface - yes. On upper surface, probably not at low angles	Probably	Probably, but this depends on exact airfoil shape	Probably
Coanda effect necessary to avoid separation	Mild Coanda effect needed	Strong Coanda effect needed	No	Weak Coanda effect needed	Mild Coanda effect needed
Propulsive efficiency	Good, it is believed	Limited because Coanda effect may dissipate jet	Limited by small slot size and jet deflection angle	Poor	Good
Transonic Mach number operation	Effective, rear stagnation point is well fixed	Effective, but floating rear stagnation point is a drawback	Can be effective, but basic shape is believed poor	Not normally used	Not known
Relative airfoil thickness for a given value of the peak velocity	150 percent	140 percent	100 percent	100 percent	130 percent
C_μ, C_L interaction - at constant angle of attack can jet thrust be varied without changing C_L?	Yes. C_L may be held fixed by control surface deflection as C_μ changes. C_L and circulation are well defined because the relative strengths of the two impinging jets are controlled by surface position	No. C_L is sensitive to C_μ and angle of attack (floating rear stagnation point	No	Yes. C_L may be held fixed by control surface deflection as C_μ changes	Yes. C_L may be held fixed by control surface deflection as C_μ changes. C_L and circulation are well-defined because the control surface position establishes the jet flow direction

*When configuration is changed to that of an augmented flap.

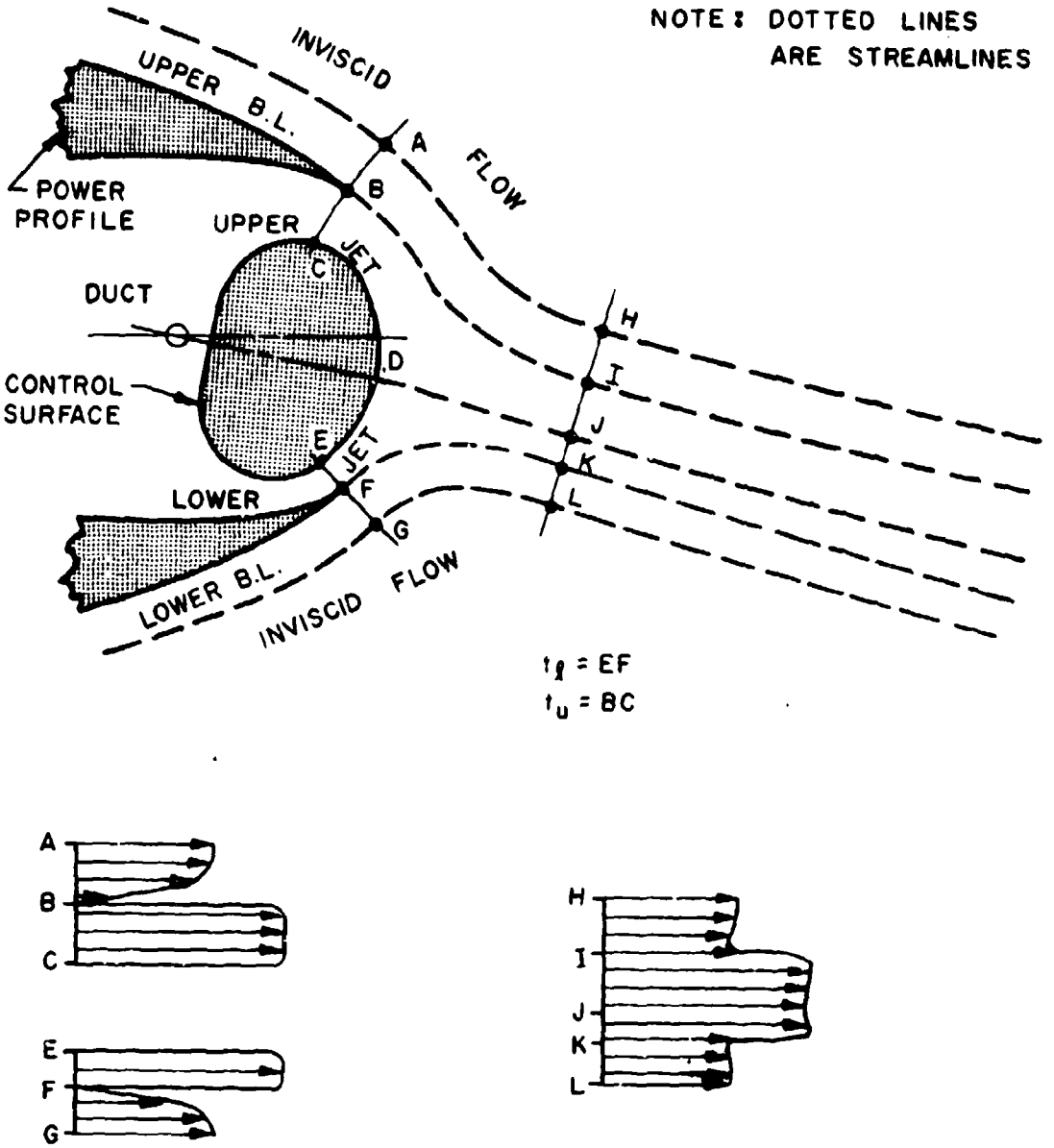

Figure 2. Sketch of the flow field near the trailing edge of a Power Profile.

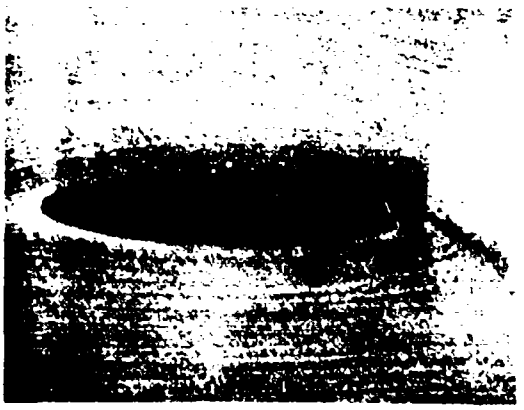

Overall View with $C_{\mu_\ell} = 0.14$ and $C_{\mu_u} = 0.6$

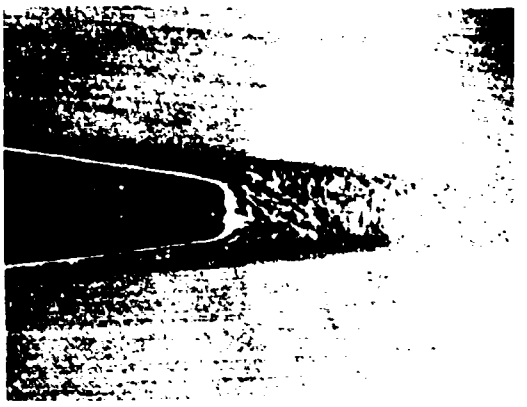

View with Trailing Edge Separation Since $C_{\mu_\ell} = C_{\mu_u} = 0$

Trailing Edge Region with $C_{\mu_\ell} = 0.14$ and $C_{\mu_u} = 0.6$

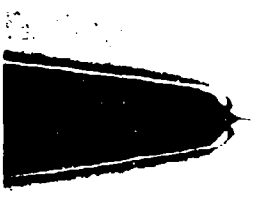

Trailing Edge Region with $C_{\mu_\ell} = C_{\mu_u} = 0.3$

Figure 3

Above: Water-Tunnel Flow Visualization Pictures of Two-Jet Airfoil Tested by Werle.

Right: Line Drawing of Trailing Edge Region Showing:

1. Streamlines
2. Equal-Velocity Lines
3. Small Separation Zone Formed by the Merger of the Two Jets.

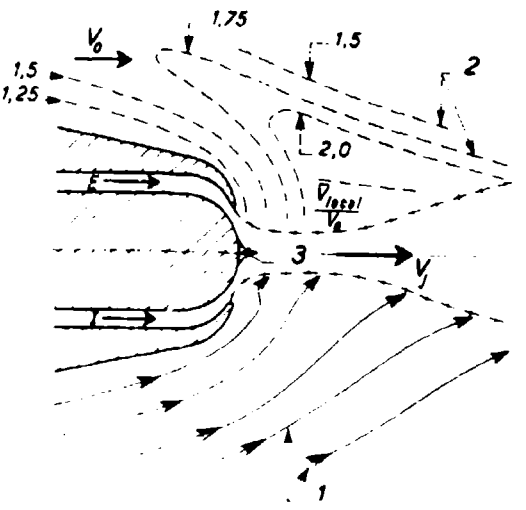

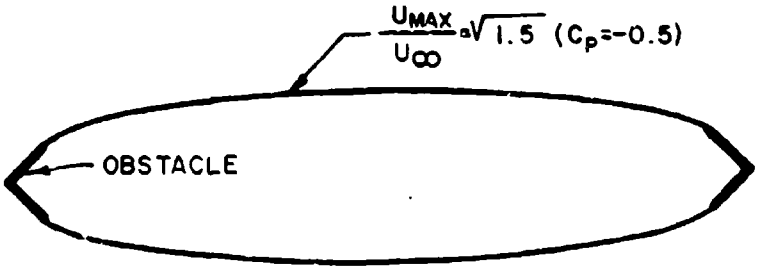

Figure 4. A 45° wedge free-streamline shape.

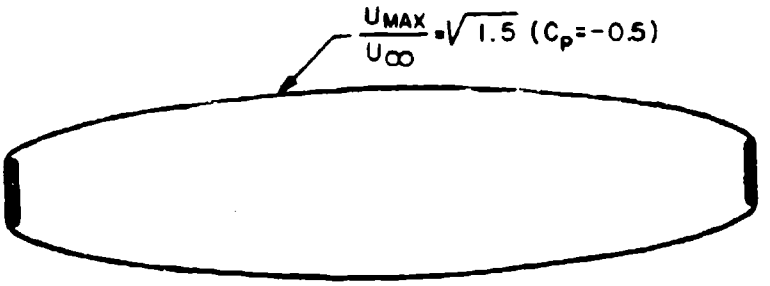

Figure 5. A 90° wedge free streamline shape.

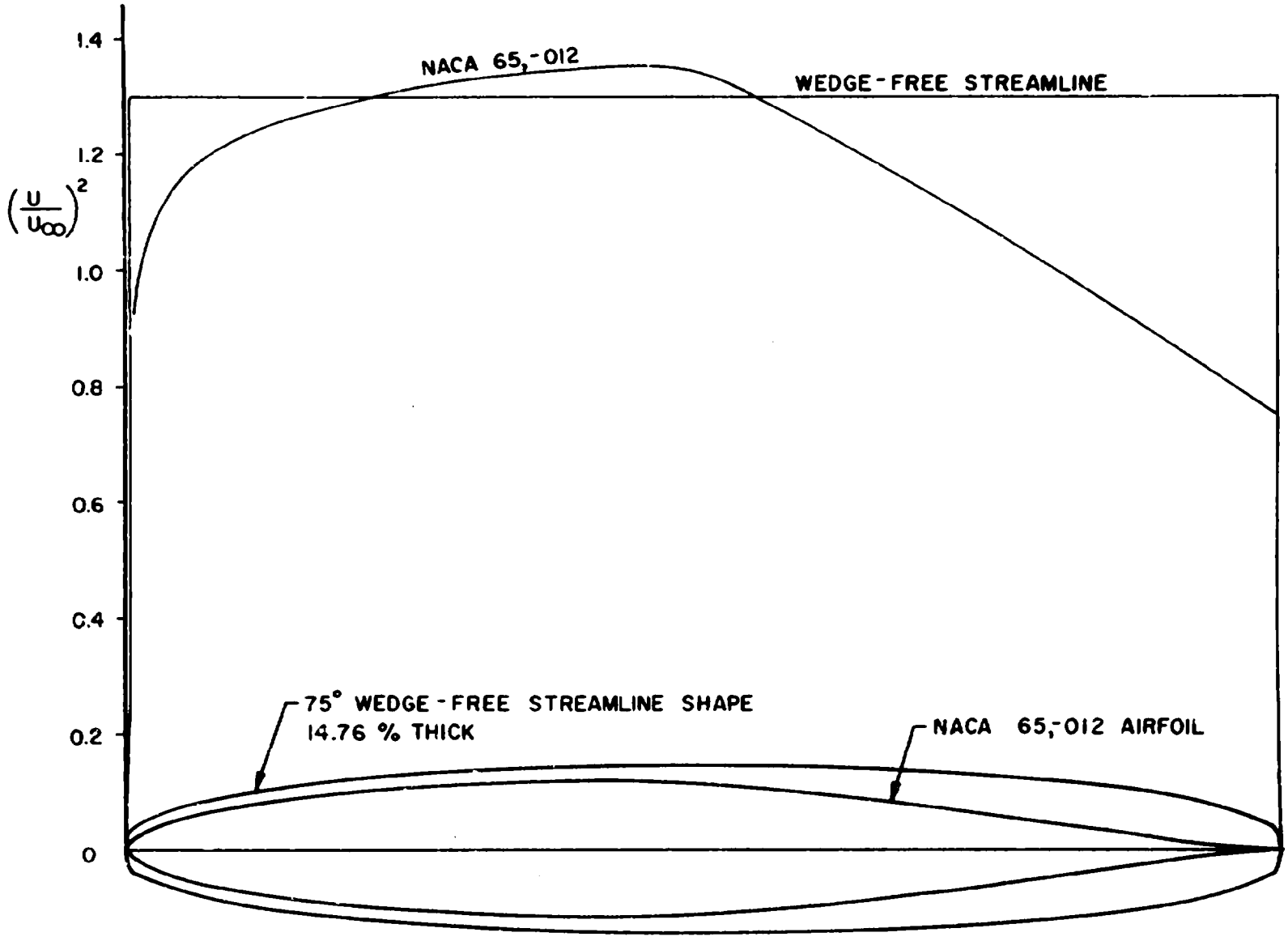

Figure 6. A comparison of the velocity distributions and the thickness distributions on an airfoil and on a free-streamline shape in inviscid, incompressible flow.

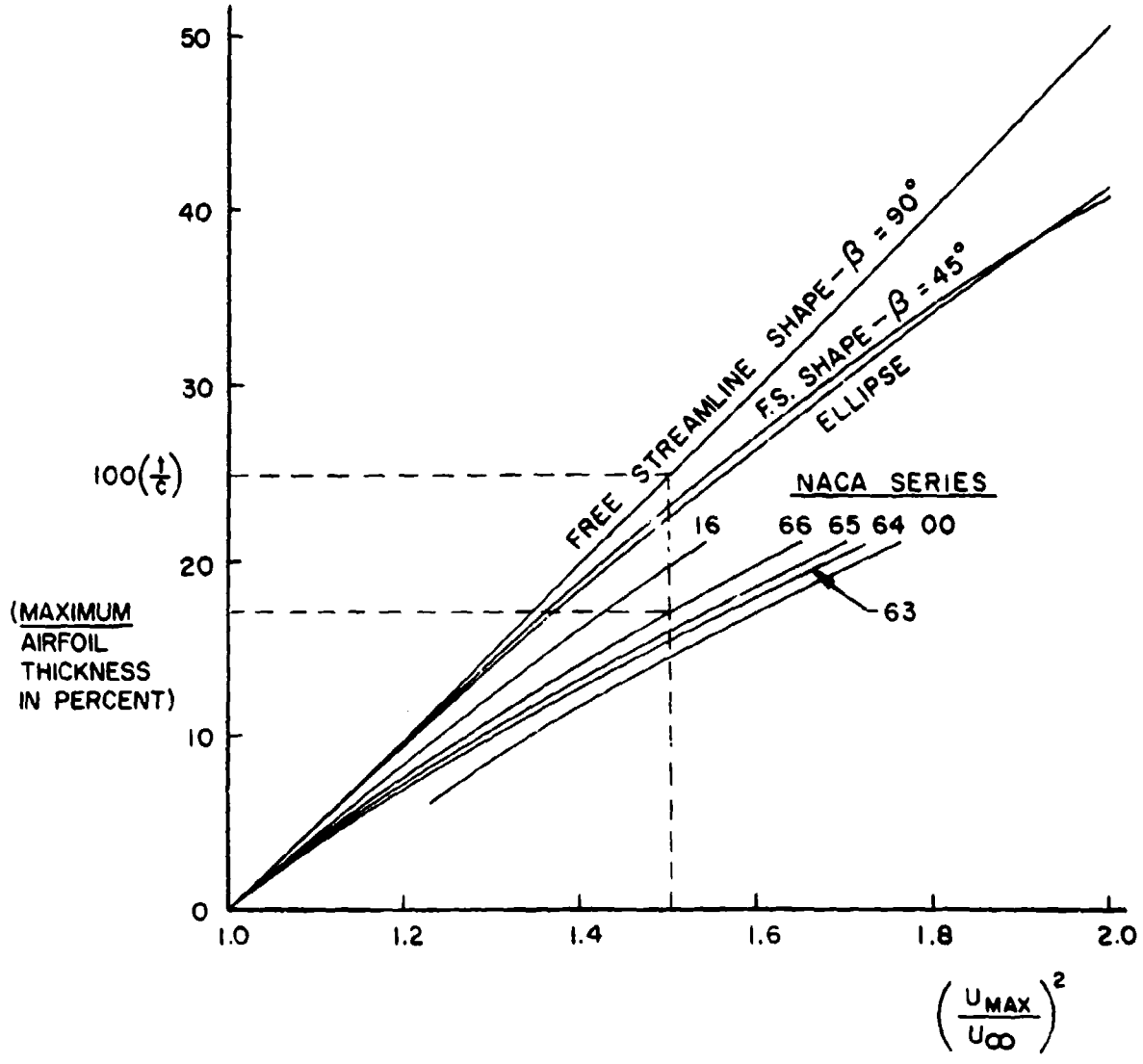

Figure 7. Maximum superstream velocity versus maximum thickness for various families of airfoils and two-dimensional shapes. Dotted lines apply to example given on page 10.

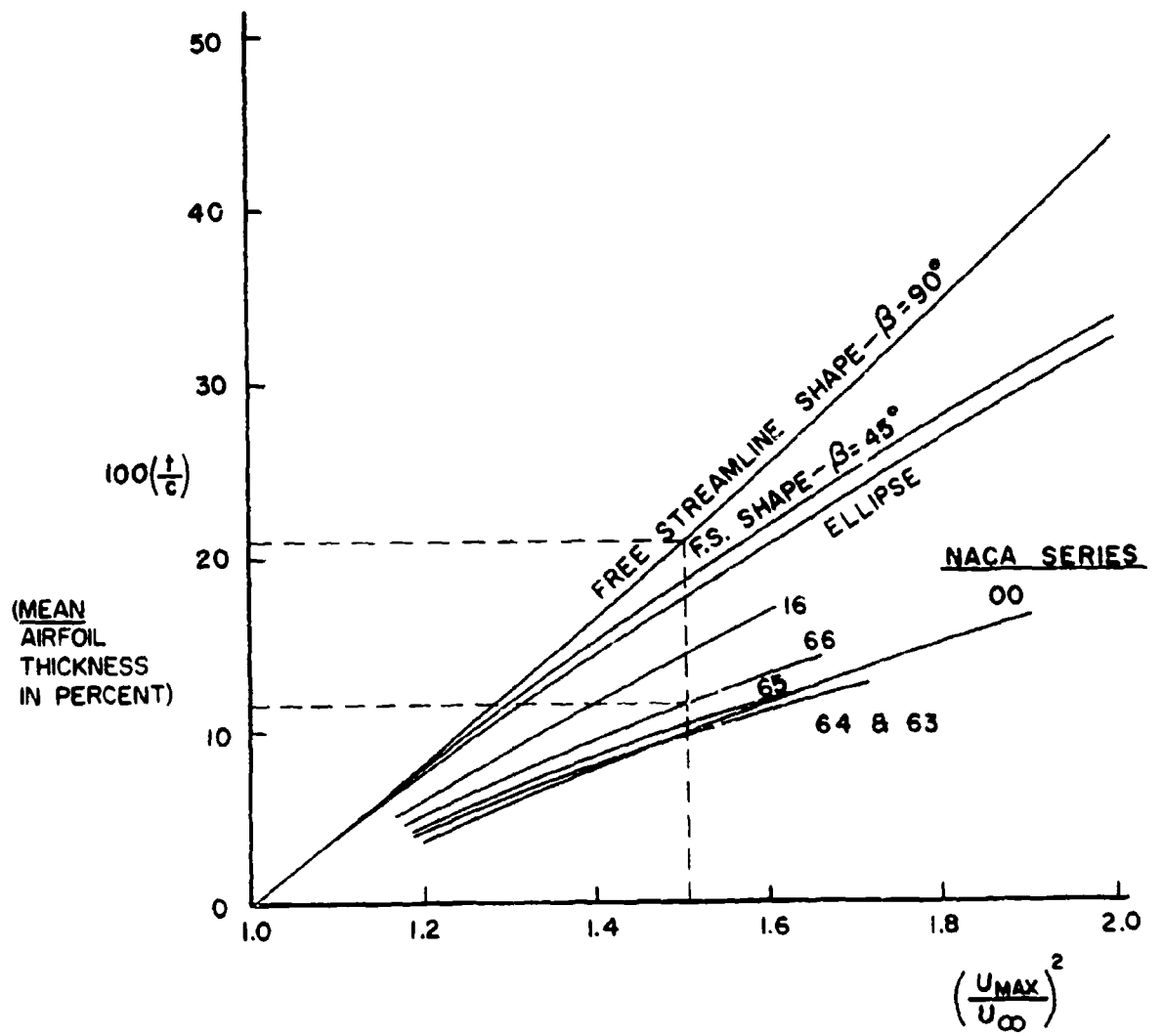

Figure 8. Maximum superstream velocity versus mean thickness for various families of airfoils and two-dimensional shapes. Dotted lines apply to example given on page 10.

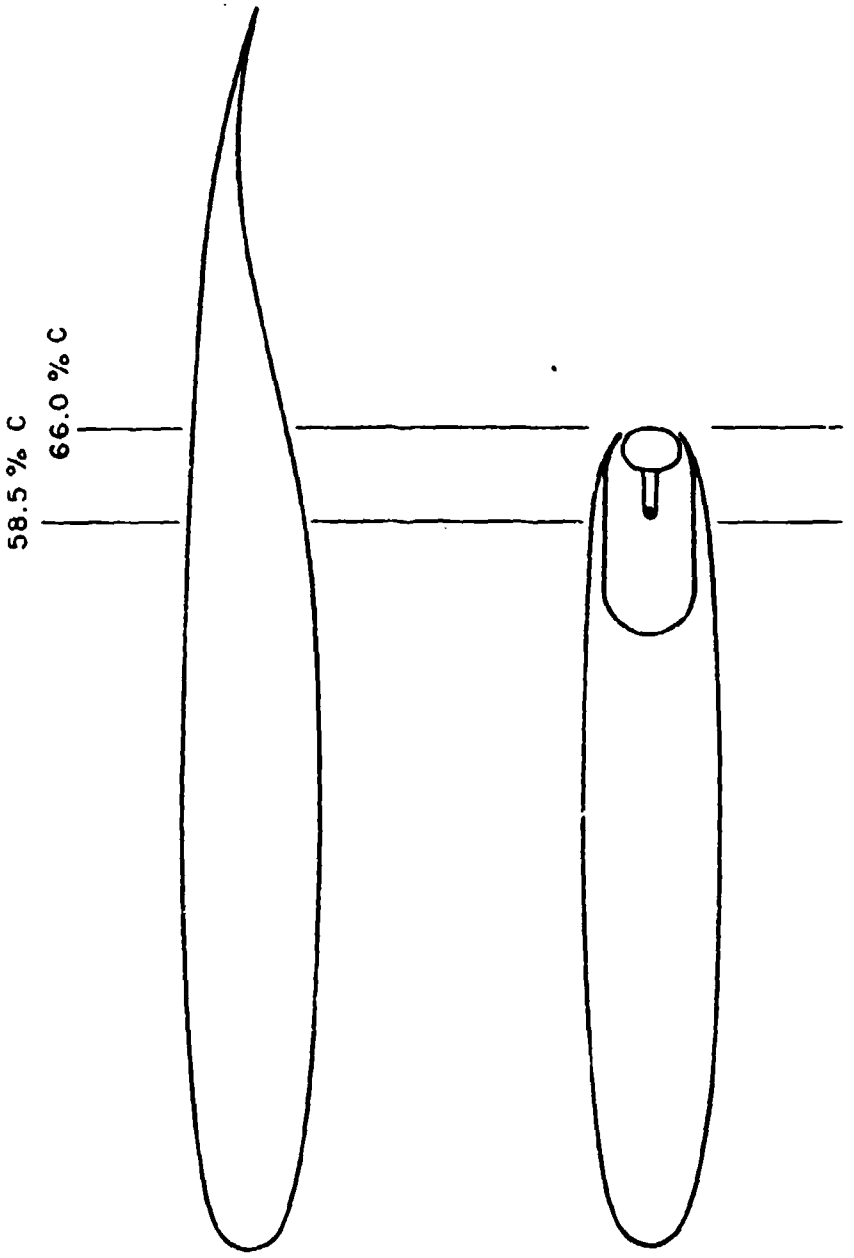

Figure 9. Comparison of a Whitcomb airfoil and a Power Profile

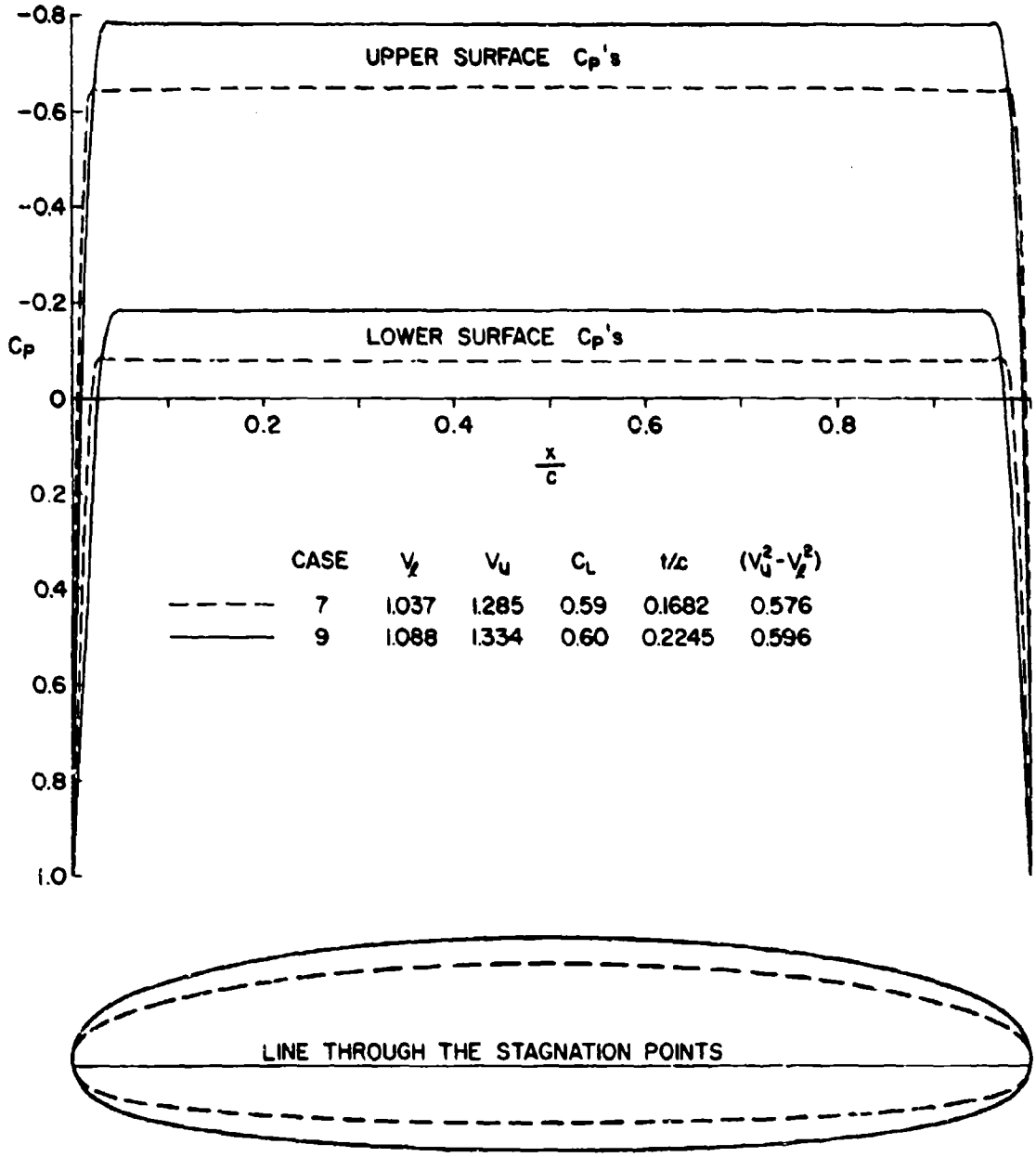

Figure 10. Two airfoil shapes and their pressure distributions as generated by the James design (inverse) method for $\alpha = 0°$.

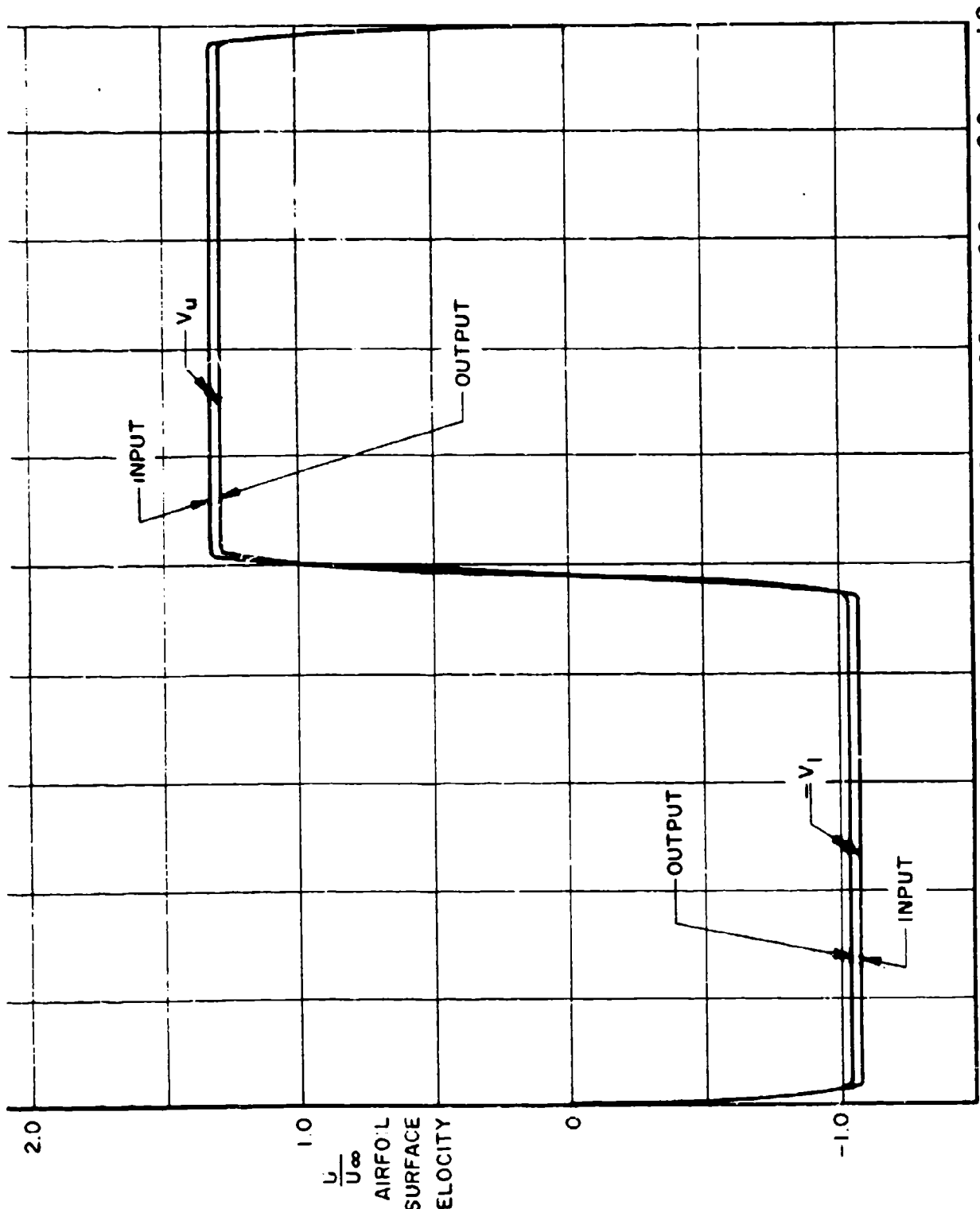

Figure 11. Airfoil Velocity Distribution for Case 7

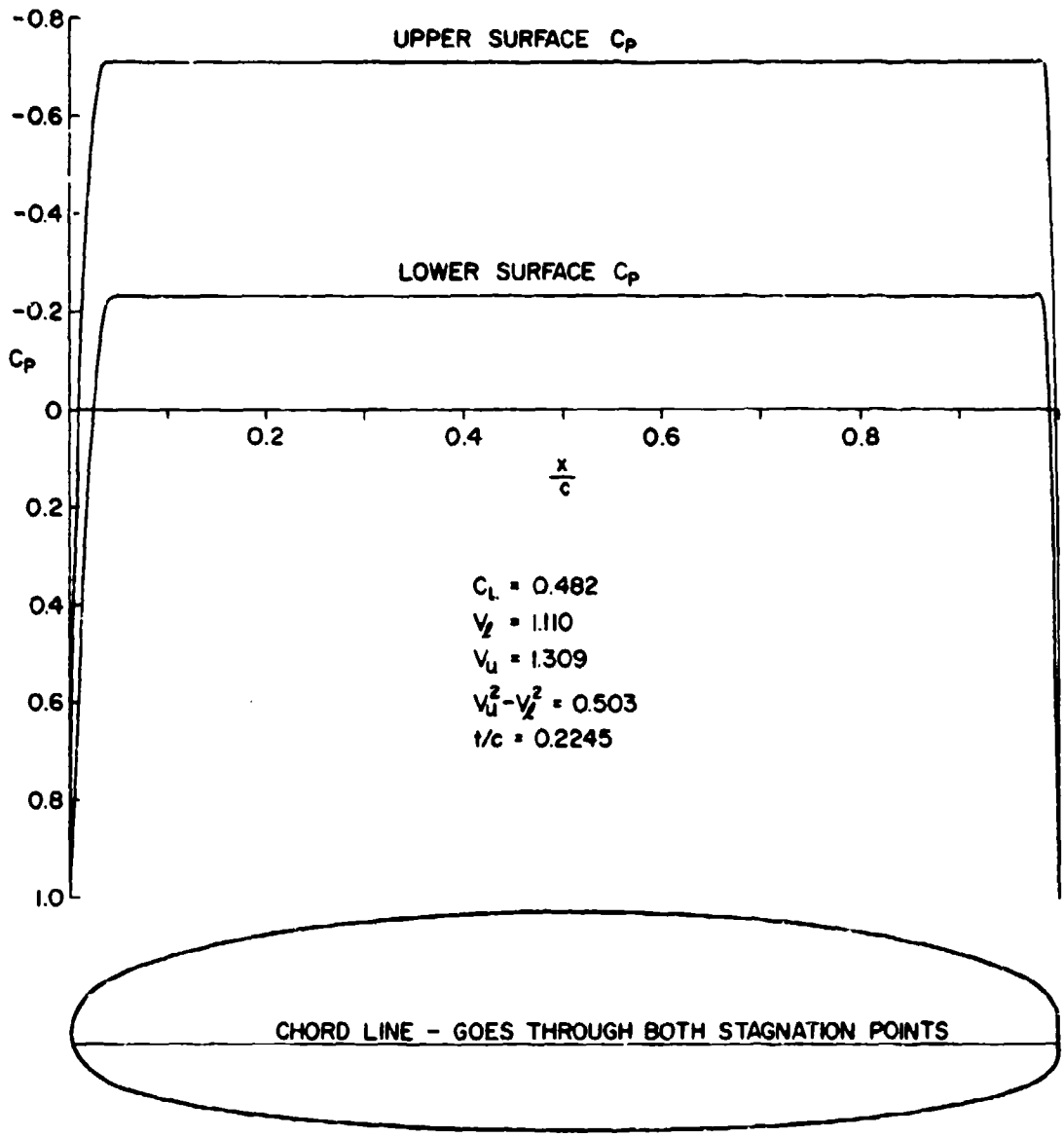

Figure 12. Final airfoil shape as generated by the James design method, $\alpha = 0^\circ$

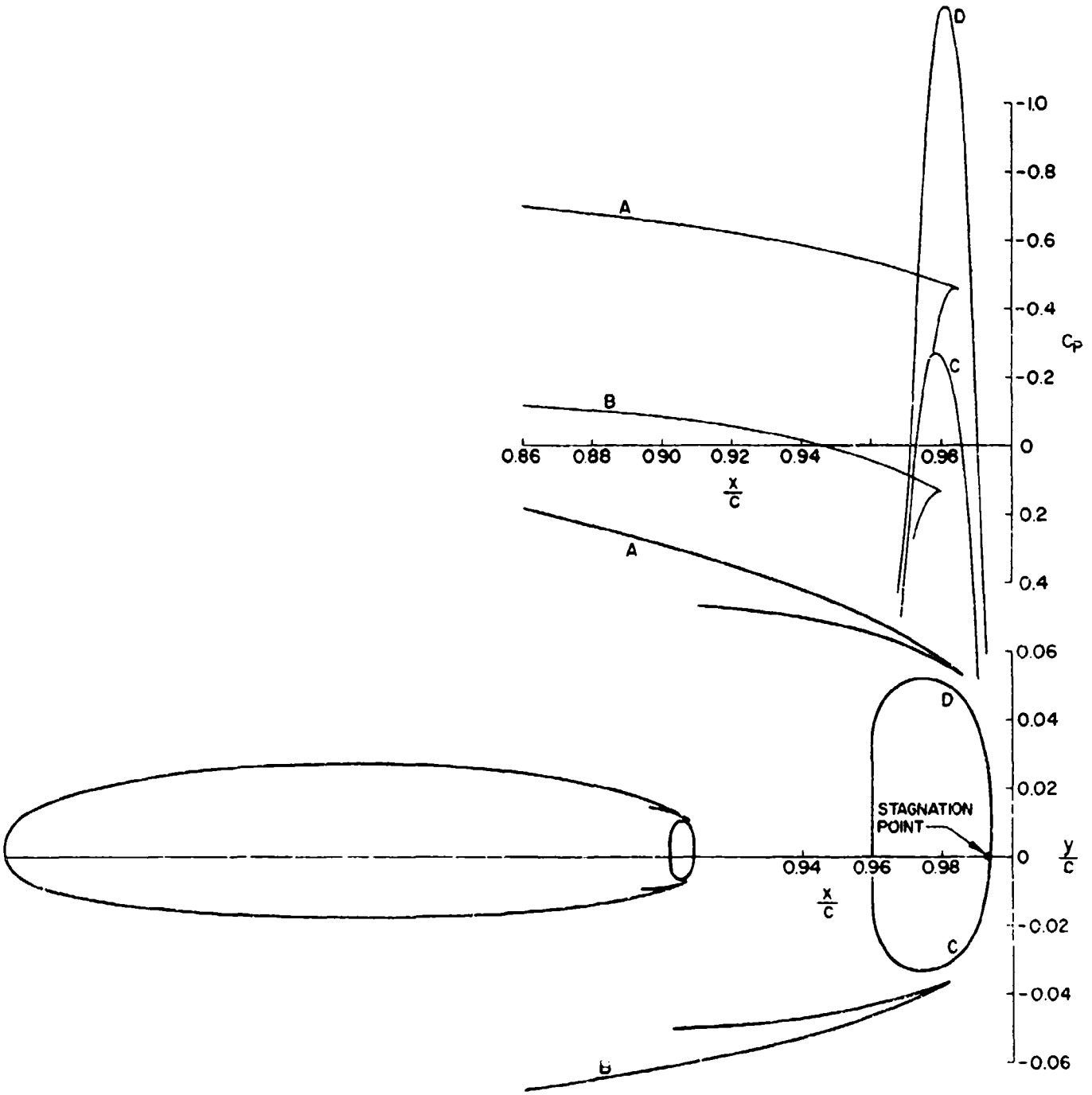

Figure 13. Final shape for Power Profile airfoil and one control surface with enlarged view of the trailing edge region showing the pressure distribution calculated by the Douglas Neumann inviscid program, $\alpha = 0^{o}$, $C_L = 0.58$.

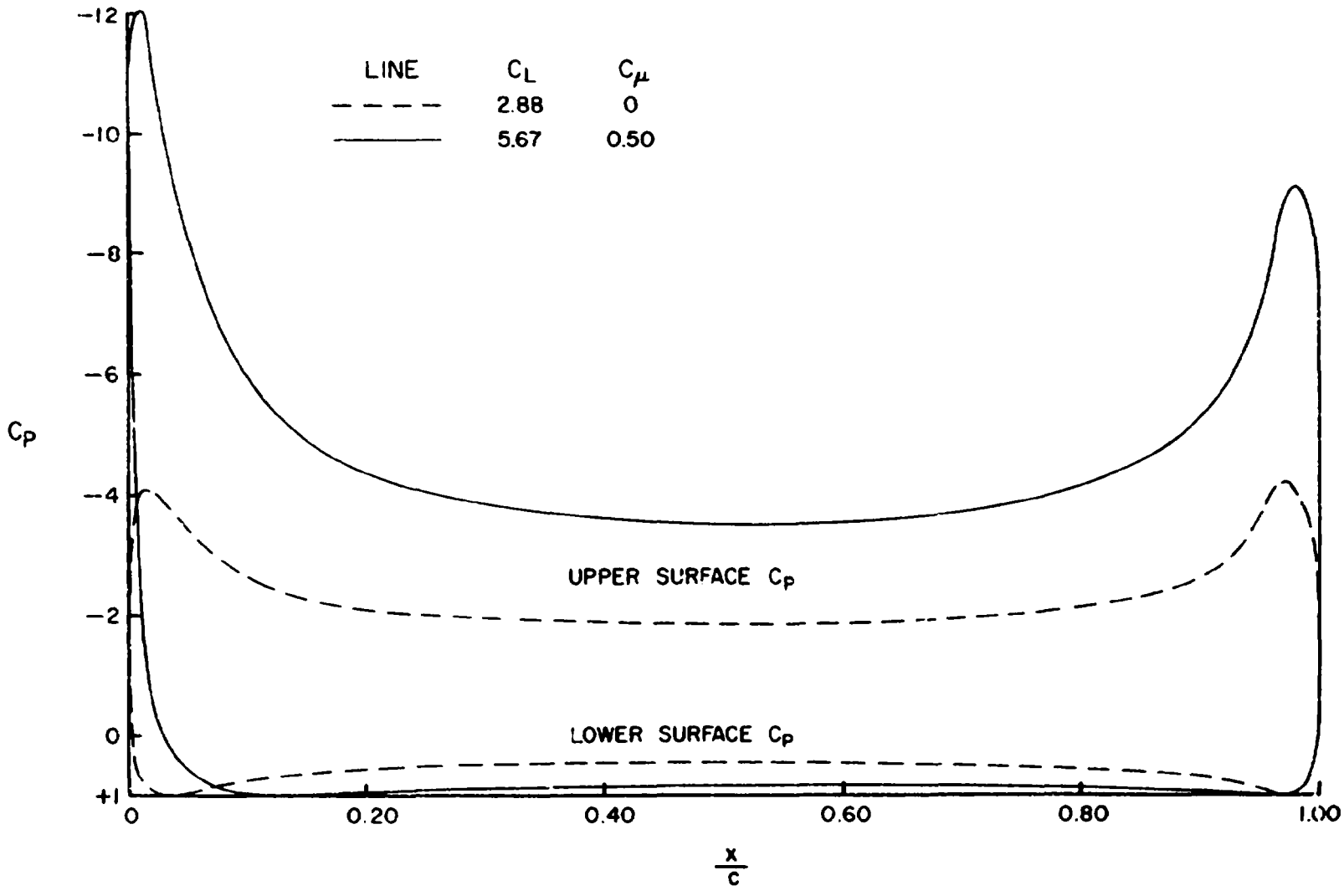

Figure 14

Pressure distribution on final airfoil shape as calculated by the Douglas Non-Linear "Jet Flap" Method. The jet is located at x/c = 0.9800 and y/c = - 0.0376. The jet initial angle is 60° downward, = 0°

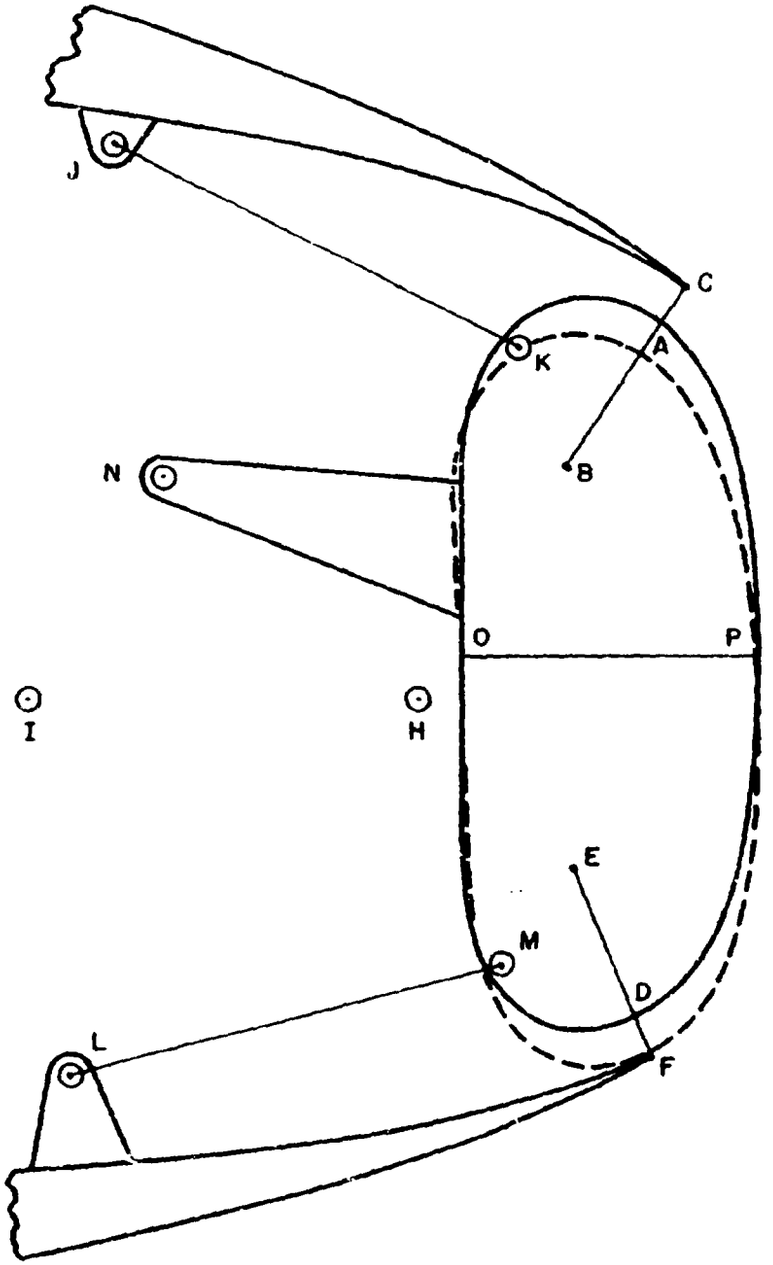

NOTE: DOTTED LINES SHOW THE CONTROL SURFACE IN THE FULL DOWN POSITION.

Figure 15

Sketch showing how the control surface motion may be constrained by links JK and LM to give an effective center of rotation about point G

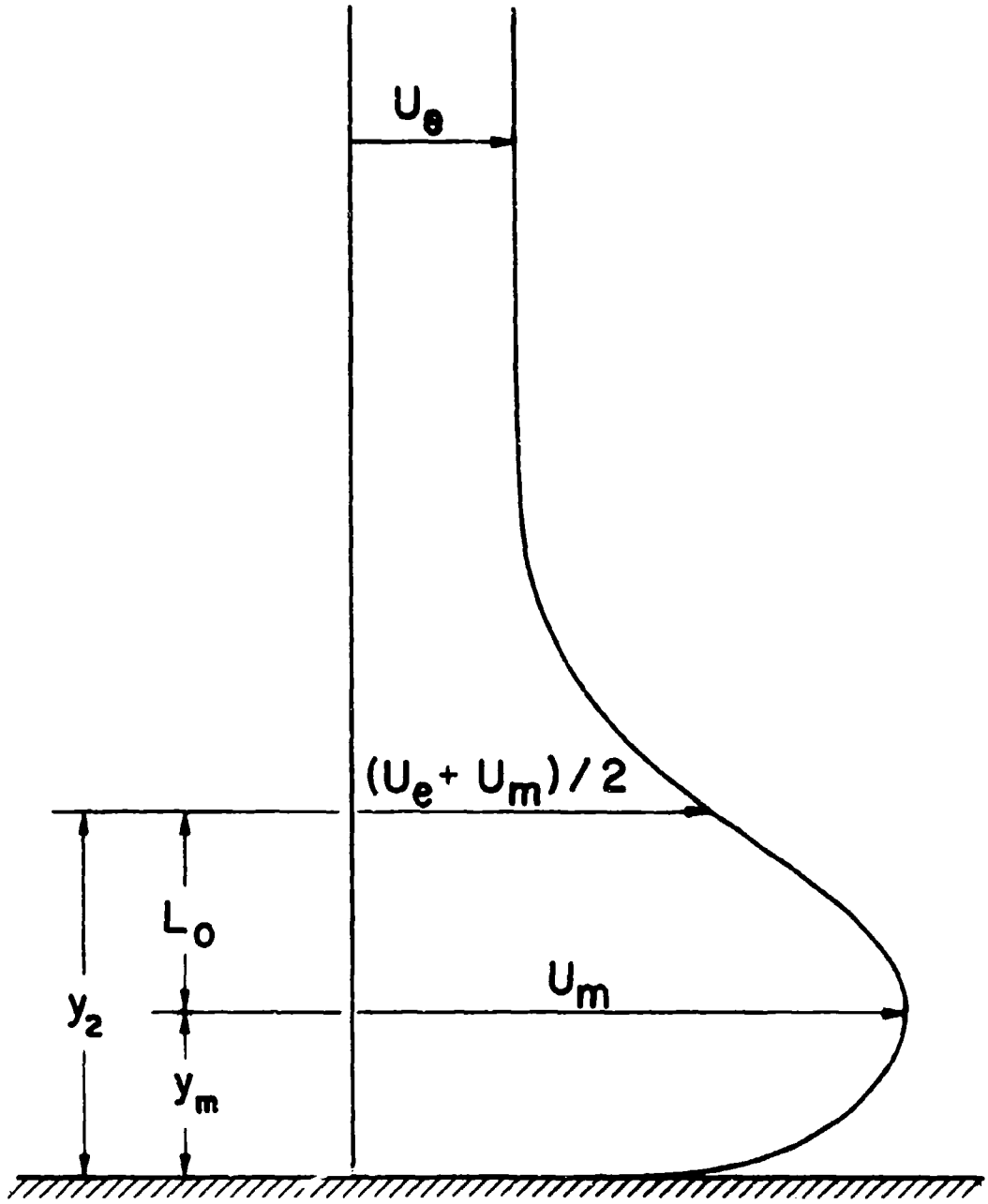

Figure 16

Wall-jet velocity profile parameters
used in the Gartshore-Newmann method

Figure 17

Wall-jet calculations by method of Gartshore and Newman

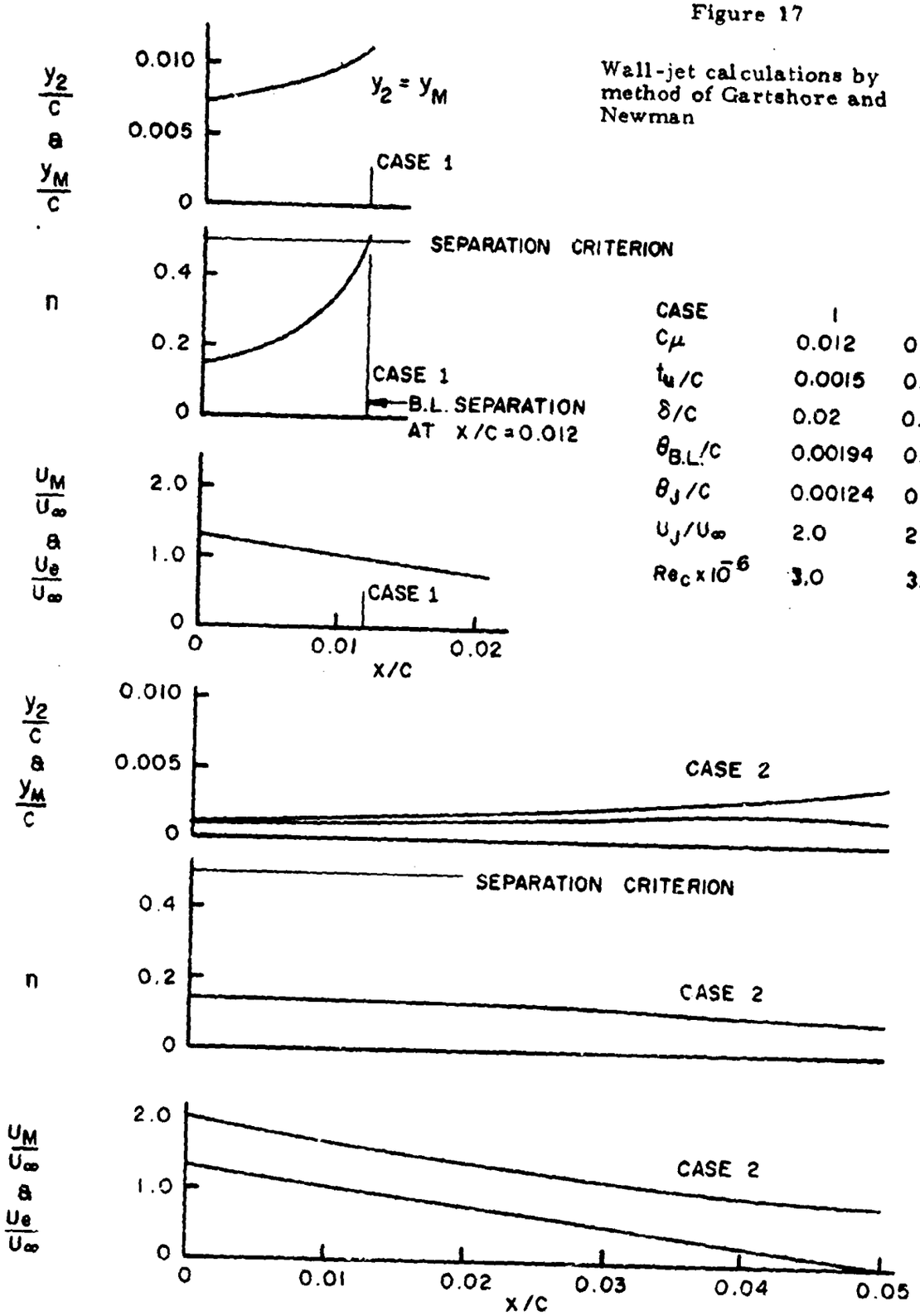

CASE	1	2
C_μ	0.012	0.024
t_u/C	0.0015	0.0030
δ/C	0.02	0.02
$\theta_{B.L.}/C$	0.00194	0.00194
θ_J/C	0.00124	0.00248
U_J/U_∞	2.0	2.0
$Re_C \times 10^{-6}$	3.0	3.0